Extrafollicular B cell activation by marginal zone dendritic cells drives T cell–dependent antibody responses

Craig P. Chappell, Kevin E. Draves, Natalia V. Giltiay, and Edward A. Clark

Department of Immunology, University of Washington, Seattle, WA 98195

Dendritic cells (DCs) are best known for their ability to activate naive T cells, and emerging evidence suggests that distinct DC subsets induce specialized T cell responses. However, little is known concerning the role of DC subsets in the initiation of B cell responses. We report that antigen (Ag) delivery to DC-inhibitory receptor 2 (DCIR2) found on marginal zone (MZ)–associated CD8α^- DCs in mice leads to robust class-switched antibody (Ab) responses to a T cell–dependent (TD) Ag. DCIR2$^+$ DCs induced rapid up-regulation of multiple B cell activation markers and changes in chemokine receptor expression, resulting in accumulation of Ag-specific B cells within extrafollicular splenic bridging channels as early as 24 h after immunization. Ag-specific B cells primed by DCIR2$^+$ DCs were remarkably efficient at driving naive CD4 T cell proliferation, yet DCIR2–induced responses failed to form germinal centers or undergo affinity maturation of serum Ab unless toll-like receptor (TLR) 7 or TLR9 agonists were included at the time of immunization. These results demonstrate DCIR2$^+$ DCs have a unique capacity to initiate extrafollicular B cell responses to TD Ag, and thus define a novel division of labor among splenic DC subsets for B cell activation during humoral immune responses.

CORRESPONDENCE
Craig P. Chappell:
cpchapp@u.washington.edu

Abbreviations used: Ab, antibody; AFC, Ab-forming cell; Ag, antigen; CLR, C-type lectin receptor; CSR, class-switch recombination; DCAL2, DC-associated lectin 2; DCIR2, DC-inhibitory receptor 2; GC, germinal center; HEL, hen egg lysozyme; MZ, marginal zone; NP, (4-hydroxy-3-nitrophenyl)acetyl; NP-CGG, NP–chicken gamma globulin; pDC, plasmacytoid DC; p.i., post-immunization; pU/UC, polyU/C RNA; TD, T cell–dependent; TI, T cell–independent; TLR, toll-like receptor.

Upon recognition of T cell–dependent (TD) or T cell–independent (TI) antigen (Ag), B cells differentiate into short-lived antibody (Ab)-forming cells (AFCs), which are critical for providing frontline protection against the spread of blood-borne pathogens such as *Salmonella typhimurium* and influenza (Gerhard et al., 1997; Cunningham et al., 2007; Rothaeusler and Baumgarth, 2010). Alternatively, cognate interaction of B cells with CD4$^+$ T cells results in the formation of germinal centers (GCs) and selection of high-affinity clones for differentiation to memory B cells and long-lived plasma cells (Jacob et al., 1991). Although GC responses and affinity maturation have been extensively studied, much less is known concerning the early events that govern B cell activation and how they influence the decision to produce extrafollicular AFC responses versus GC B cell differentiation.

The context in which B cells encounter Ag is highly influenced by the size, nature, and form of the Ag itself (Roozendaal et al., 2009). Although direct recognition of small, soluble Ag by the BCR can occur in vivo

(Pape et al., 2007), acquisition of membrane-associated Ag is also an efficient means to trigger B cell activation (Carrasco and Batista, 2006; Depoil et al., 2008). Multiple APCs can present Ag to B cells including follicular DCs, subcapsular sinus and marginal zone (MZ) macrophages, and DCs (Wykes and MacPherson, 2000; Huang et al., 2005; Qi et al., 2006; Phan et al., 2009; Roozendaal et al., 2009; Suzuki et al., 2009). Among these, DCs in particular have been shown in vitro to influence a range of B cell processes including proliferation, differentiation, and Ig class-switch recombination (CSR; Dubois et al., 1998; Fayette et al., 1998; Litinskiy et al., 2002; Craxton et al., 2003). DC-mediated presentation of Ag to B cells in vivo has been shown to enhance TI Ab responses to immune complexes internalized by FcγRIIb on splenic DCs, as well as TI responses against *Streptococcus pneumoniae* mediated by

The Rockefeller University Press $30.00
J. Exp. Med. 2012 Vol. 209 No. 10 1825-1840
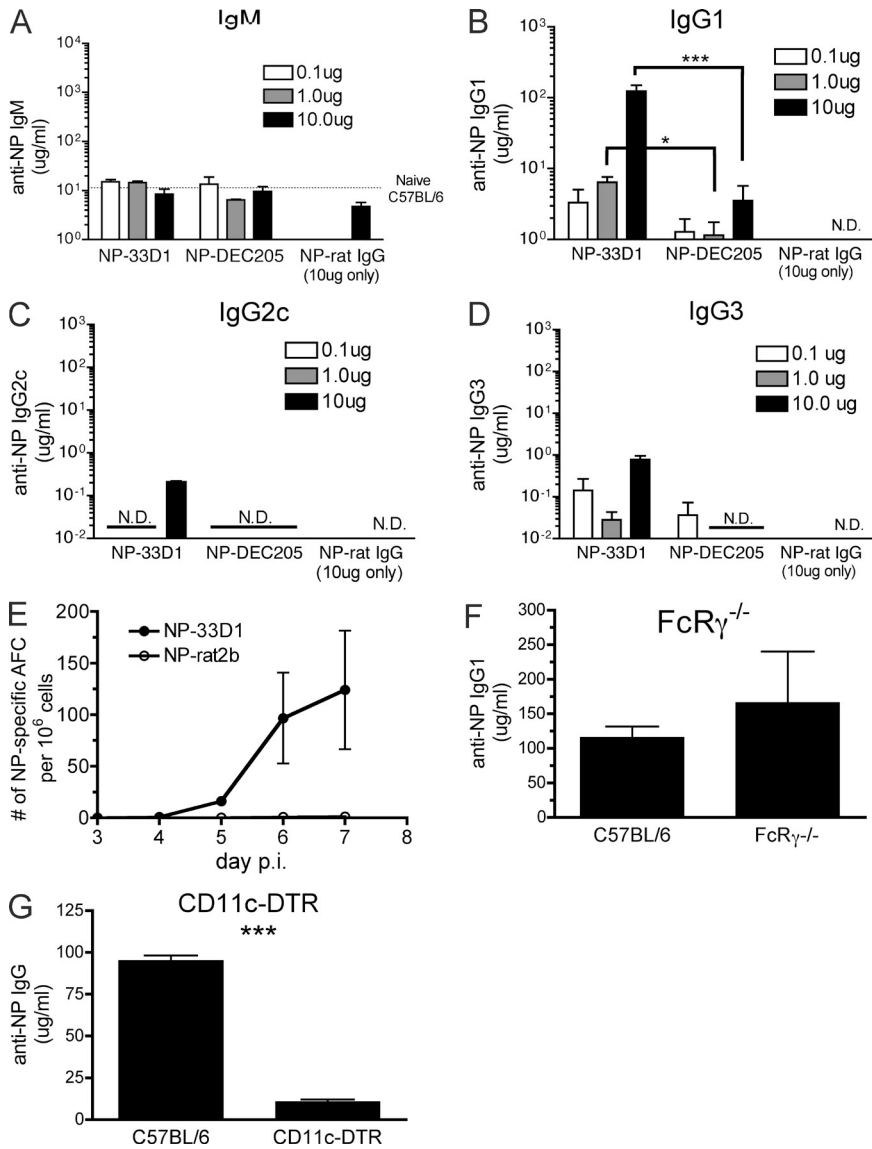www.jem.org/cgi/doi/10.1084/jem.20120774

1825

Figure 1. Ag delivery to DCIR2+ DCs in vivo induces IgG1–restricted Ab responses. (A–D) ELISA analyses of NP-specific serum Ab from B6 mice immunized 10 d earlier with the indicated dose of NP-33D1, NP-DEC205, or NP-rat IgG. Graphs show the mean ± SEM of a representative experiment from three independent experiments using three to four mice/group (using the 10 µg dose). Data were analyzed by two-way ANOVA analysis. (E) ELISPOT analysis showing the number of IgG-secreting NP-specific AFCs in the spleens of C57BL/6 mice on the days indicated after administration of NP-33D1 or NP-rat2b. The mean ± SEM from a single experiment using four mice/group/day is shown. (F) Day 10 anti-NP IgG1 Ab responses in FcγRγ-deficient and C57BL/6 mice immunized with NP-33D1. (G) Day 10 anti-NP IgG1 Ab responses in CD11c-DTR transgenic and C57BL/6 mice treated with 100 ng DT 24 h before immunization with NP-33D1. Data in F and G were analyzed by unpaired Student's t test and are representative experiments from three and two independent experiments, respectively, and show the mean ± SEM using three to four mice/group. P-value indicators *** and * refer to $P < 0.001$ and $P < 0.05$, respectively.

(F4/80-like receptor), CIRE (C-type lectin immune receptor), Dectin-1, Clec12a, and Clec9a (Corbett et al., 2005; Caminschi et al., 2008; Lahoud et al., 2009). Because the CLRs targeted in these studies are also expressed on macrophages, plasmacytoid DCs (pDCs), and/or B cells, it is again unclear which APC populations were required for the observed Ab induction. In sum, many questions remain concerning the induction of Ab responses by DCs.

blood-derived DCs (Balázs et al., 2002; Bergtold et al., 2005; Dubois and Caux, 2005).

In contrast, it is unclear what, if any, role DC–B cell interactions may have during humoral responses to TD Ag. Some evidence has suggested that DCs directly present Ag to B cells during TD immune responses. Qi et al. (2006) showed that adoptively transferred DCs can transfer hen egg lysozyme (HEL) to Ag-specific B cells in the lymph node; however, neither the DC subset responsible for the Ag presentation nor the subsequent B cell response was evaluated. Earlier studies showed that adoptive transfer of Ag-bearing DCs was sufficient to induce TD Ab responses; however, because adoptive transfer strategies were used, the role of Ag uptake in situ by resident DC subsets remained unclear (Wykes et al., 1998; Berney et al., 1999). More recent studies using mAbs to deliver Ag directly to APCs in vivo demonstrated Ab responses after Ag uptake by several C-type lectin receptors (CLRs) including FIRE

Here, we describe a novel mechanism underlying DC-mediated induction of Ab responses after Ag uptake by DC-inhibitory receptor 2 (DCIR2), a CLR found exclusively on a subset of MZ-associated CD8α− DCs (Dudziak et al., 2007). Using mAbs to deliver Ag in vivo, we show that Ag uptake by DCIR2, but not DEC205 found on CD8α+ DCs, induces robust IgG1-restricted TD Ab responses without the addition of any adjuvant. Although DCIR2+ DCs are known to preferentially present peptide–MHCII complexes to CD4 T cells after Ag delivery to DCIR2 (Dudziak et al., 2007), we found that DCIR2+ DCs also present Ag to B cells and facilitate their rapid activation in vivo. As early as 24 h after immunization, activated Ag-specific B cells accumulated in extrafollicular splenic bridging channels, coincident with the location of DCIR2+ DCs in situ. Importantly, DC-primed Ag-specific B cells were highly efficient APCs for driving naive CD4 T cell
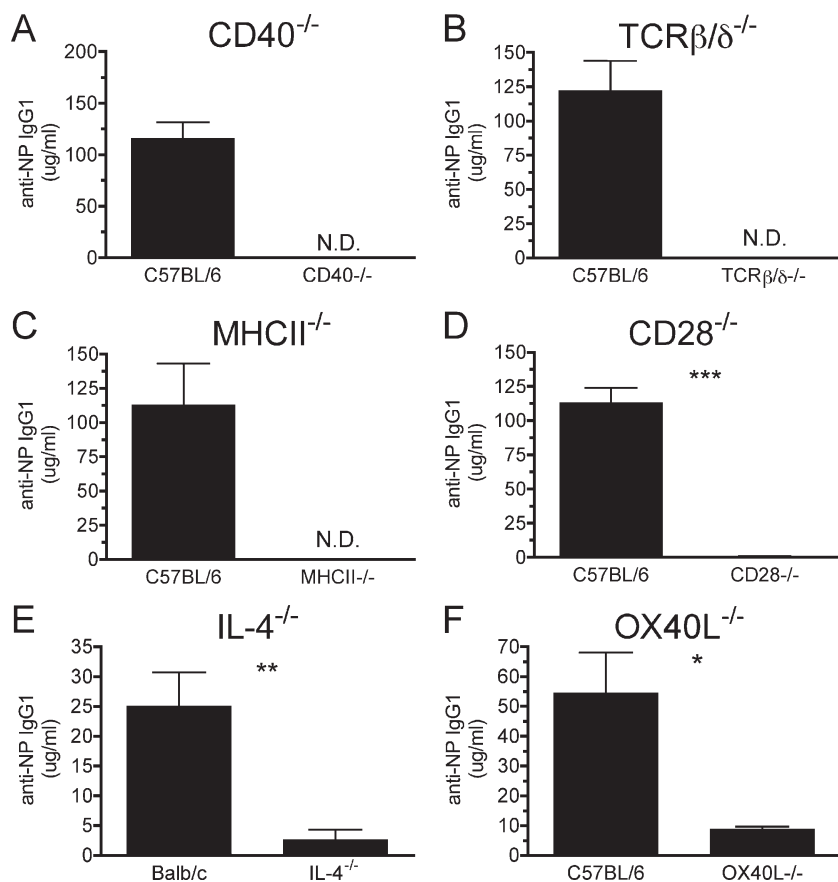
Figure 2. DCIR2–induced Ab responses are TD. Groups of C57BL/6 (A–D and F) or BALB/c animals (E) and mice deficient in the indicated gene product were immunized with NP-33D1 and bled 10 d later for serum Ab analysis by ELISA. Graphs depict the mean ± SEM of anti-NP IgG1 serum Ab. Data in A, B, and E are representative data from three independent experiments each. Data in C, D, and F are representative of two independent experiments each. All experiments used three to five mice/group and were analyzed by unpaired Student's t tests. N.D. = not detected. P-value indicators ***, **, and * refer to P < 0.001, P < 0.01, and P < 0.05, respectively.

(NP-DEC205), or to nonspecific poly-clonal rat IgG (NP-rat IgG), and administered graded doses (0.1–10 µg) i.v. to groups of C57BL/6 (B6) mice. Animals immunized with NP-33D1, NP-DEC205, or NP-rat IgG failed to produce anti-NP IgM Abs at all doses tested (Fig. 1 A). In contrast, mice injected with NP-33D1 produced dose-dependent increases in anti-NP IgG1 Ab that exceeded those induced by NP-DEC205 up to 35-fold (for the 10 µg dose; Fig. 1 B). Anti-NP Ab induced by NP-33D1 was almost exclusively IgG1, with little to no IgG2c or IgG3 (Fig. 1, C and D). IgG-secreting NP-specific AFCs were first detectable on day 4 post-immunization (p.i.) and continued to increase through day 7 (Fig. 1 E). Ag uptake by DCIR2 was required because anti-NP Abs were not detected after injection of nonspecific NP-rat IgG (Fig. 1, A–D), and equivalent or greater responses were obtained in FcRγ-deficient mice compared with B6 controls after NP-33D1 administration (Fig. 1 F). Finally, as expected, depletion of CD11c+ cells using B6 CD11c-DTR mice significantly abrogated the Ab response to NP-33D1 (Fig. 1 G), demonstrating the DC dependence of DCIR2-induced responses.

DC-derived BAFF (B cell activating factor) and/or APRIL (a proliferation-inducing ligand) can induce CD40-independent CSR (Litinskiy et al., 2002). However, we detected no NP-specific IgG1 after immunization of CD40-deficient animals with NP-33D1 (Fig. 2 A). Interestingly, this lack of IgG1 Ab was not accompanied by increases in IgM or IgG2c (unpublished data). Furthermore, Ab responses were absent after NP-33D1 immunization of mice deficient in TCR-β/δ chains, MHCII, or CD28 (Fig. 2, B–D). Thus, cognate Ag presentation to CD4 T cells is an absolute requirement for DCIR2-induced Ab responses.

The predominance of IgG1 Ab suggested that NP-33D1 induced T_H2-driven Ab responses. Anti-NP Ab responses driven by NP-33D1 immunization were significantly reduced in IL-4–deficient animals, which was not accompanied by

proliferation, suggesting that B cell–mediated Ag presentation is a key component to sustaining CD4 T cell responses after Ag delivery to DCs. In the absence of adjuvants, DCIR2 DCs induced extrafollicular Ab responses that did not involve GC formation or affinity maturation of serum Ab. Instead, inclusion of agonists for toll-like receptor (TLR) 7 or TLR9 (but not TLR3, TLR5, or RIG-I) shifted the B cell differentiation program toward GC formation and affinity maturation. Thus, our data show that DCIR2+ MZ-associated DCs are uniquely equipped and/or positioned to prime B cells and initiate extrafollicular Ab responses to TD Ag.

RESULTS
MZ–associated DCIR2+ DCs induce robust TD Ab responses
Conventional splenic DCs in mice can be subdivided into two broad subsets: CD11c+CD8α+ DCs that express DEC205 (CD205) and CD11c+CD8α− cells, most of which express DCIR2 (recognized by the mAb 33D1; Dudziak et al., 2007; Kasahara and Clark, 2012). Previous studies showed that delivery of Ag to these DC subsets is achieved by coupling Ag to mAbs directed against DEC205 or DCIR2 (Dudziak et al., 2007). To determine whether these DCs differ in their ability to induce Ab responses after Ag uptake, we coupled the hapten (4-hydroxy-3-nitrophenyl) acetyl (NP) to mAbs against DCIR2 (NP-33D1) or DEC205
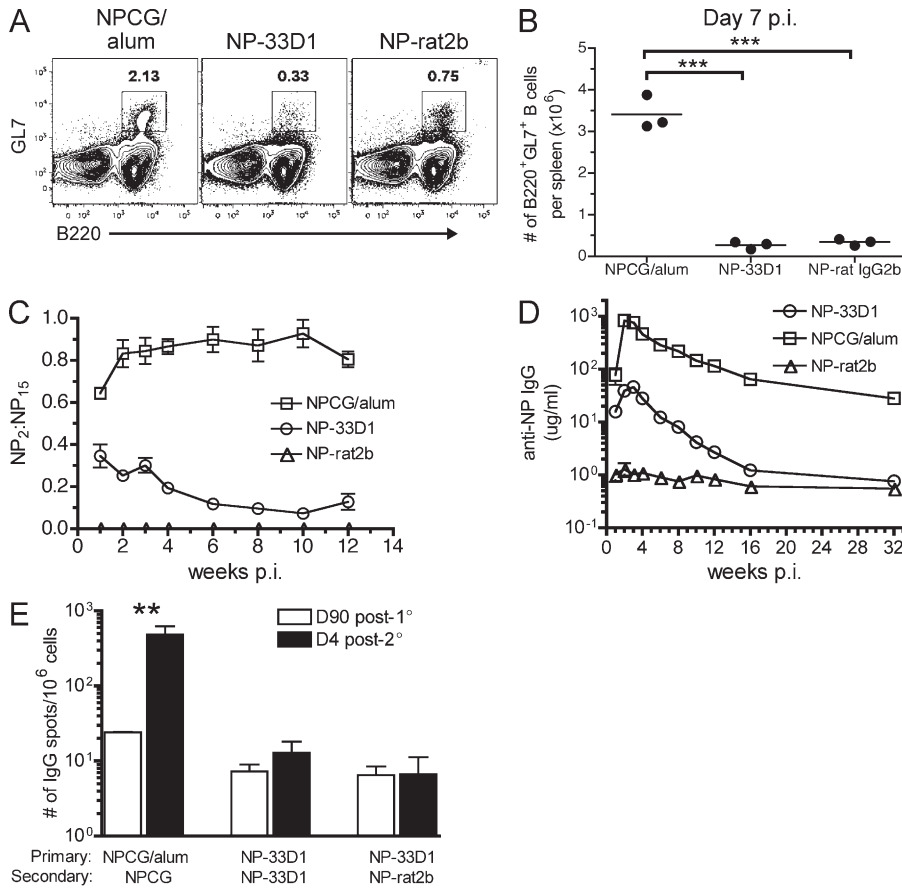
Figure 3. Ag delivery to DCIR2+ DCs does not induce GC formation, affinity maturation, or long-lived Ab responses and fails to prime for Ag recall. (A) Flow cytometry plots show the frequency of splenic B220+GL7+ GC B cells in C57BL/6 mice immunized 7 d previously with 50 µg NP-CGG plus alum or 10 µg NP-33D1 or NP-rat2b. (B) Total numbers of splenic B220+GL7+ GC B cells from the mice in A. Each dot represents an individual animal with the mean (horizontal bars) indicated. Data were analyzed by one-way ANOVA with Bonferroni's post-tests and are representative of three independent experiments using three to four mice/group. (C and D) Groups of C57BL/6 mice were immunized as in A, and the relative affinity (C) or quantity (D) of anti-NP IgG Ab over time was determined by ELISA. Mean ± SEM is graphed for a single experiment using four mice/group. (E) C57BL/6 mice were immunized as in A and rechallenged with 10 µg NP-CGG, NP-33D1, or NP-rat2b as indicated 90 d after primary immunization. ELISPOT analysis shows the number of NP-specific IgG AFCs recovered from spleens 4 d after challenge. Data in E were analyzed by two-way ANOVA and are representative data from two independent experiments using four mice/ group. P-value indicators *** and ** refer to P < 0.001 and P < 0.01, respectively.

an increase in anti-NP IgM or IgG2c (Fig. 2 E and not depicted). Furthermore, OX40L, which is essential for T_H2 responses (Flynn et al., 1998), was also required (Fig. 2 F). Together, these results demonstrate that Ag delivery to DCIR2 on MZ-associated DCs is sufficient to induce robust T_H2-driven Ab responses.

DCIR2+ DCs do not induce GCs or long-lived B cell responses
GCs are TD structures essential for the generation of high-affinity Ab. The requirement for T cell help during DCIR2-induced Ab responses suggested that Ag delivery to DCIR2+ DCs may evoke GC formation. However, in contrast to mice immunized with NP–chicken gamma globulin (NP-CGG) precipitated in alum, NP-33D1 immunization did not induce significant accumulation of GL7+ GC B cells by day 7 p.i. (Fig. 3, A and B). Furthermore, serum Ab recovered from mice immunized with NP-33D1 failed to undergo affinity maturation over time, whereas mice immunized with NP-CGG plus alum displayed increased and sustained high-affinity Ab responses (Fig. 3 C). NP-specific Ab titers after NP-33D1 administration did not persist and decayed to barely detectable levels over time (Fig. 3 D). Finally, unlike NP-CGG plus alum controls, mice immunized with NP-33D1 failed to mount Ag recall responses upon

rechallenge with either soluble NP-rat2b or NP-33D1 when analyzed by plasma cell ELISPOT assay 4 d after Ag rechallenge (Fig. 3 E). These results suggest that DCIR2+ DCs invoke TD extrafollicular Ab responses after Ag uptake by DCIR2.

Ligation of DCIR2 by the 33D1 mAb does not up-regulate MHCII, CD80, or CD86 on MZ DCs (Dudziak et al., 2007). Thus, we reasoned that the absence of GC formation after NP-33D1 immunization was perhaps a result of Ag presentation by immature MZ DCs. Among splenic DC subsets, DCIR2+ DCs express the highest levels of TLR5 (Kasahara and Clark, 2012), the ligand for flagellin, and have high levels of RIG-I, an intracellular RNA helicase which recognizes viral RNA (Barbalat et al., 2011). Therefore, we immunized mice with NP-33D1 or NP-rat2b together with flagellin, the RIG-I activator polyU/C RNA (pU/UC; Saito et al., 2008), or polyI:C (a TLR3 agonist) and analyzed serum Ab responses 28 d later. Each agonist modestly increased the magnitude of anti-NP Ab responses compared with NP-33D1 alone (Fig. 4, A and C) but, surprisingly, failed to induce affinity maturation of serum Ab compared with NP-rat2b plus alum (Fig. 4, B and D). Collectively, these results demonstrate that TLR3, TLR5, or RIG-I agonists do not alter the extrafollicular Ab program induced by DCIR2+ DCs.

DCIR2+ DCs mediate rapid activation of Ag–specific B cells in vivo

To better understand the mechanism by which DCIR2+ DCs induce anti-NP Ab responses, we examined early B cell activation after NP-33D1 administration. To directly monitor B cell activation, we adoptively transferred NP-specific B cells from Ly5.1+ B1-8hi knockin mice (Shih et al., 2002a) to B6 recipients 24 h before immunization with NP-33D1, NP-rat2b, or PBS (all i.v.), or with NP-rat2b plus alum (i.p.). At 24, 48, and 72 h after immunization, we analyzed B cells by flow cytometry using Ly5.1 expression and NP binding to identify the transferred Ag-specific B cells. As early as 24 h after Ag delivery, NP-specific B cells from all three groups of mice that received Ag displayed significant reductions in NP binding compared with PBS-injected controls (Fig. 5 A). Reduced Ag binding likely reflects BCR occupancy by Ag and, importantly, indicates that NP-specific B cells in each group were exposed to Ag regardless of the form (soluble vs. particulate) or route (i.v. vs. i.p.) in which it was administered. Strikingly, NP-binding B cells from mice immunized with NP-33D1 showed highly increased expression of the activation markers CD69, CD86, and MHCII compared with controls inoculated with PBS, NP-rat2b, or NP-rat2b in alum (Fig. 5, B and C). Additionally, the follicular homing receptor CXCR5 was down-regulated on NP-binding B cells from NP-33D1–immunized mice compared with controls (Fig. 5, B and C), and CCR7 levels were elevated (Fig. 5 C), suggesting that these cells were no longer present within B cell follicles. We detected no changes in expression of CXCR4, CD40, CD80, or OX40L 24 h p.i. among B cells from NP-33D1 immunized mice (unpublished data). This activation profile remained essentially unchanged at 48 and 72 h p.i. with the notable exception of OX40L, which was strongly up-regulated on B cells at both 48 and 72 h (Fig. 5 D).

In contrast to NP-binding B cells, Ly5.1+ NP-negative (i.e., nonspecific) B cells from NP-33D1–immunized mice failed to increase their expression of activation markers or decrease expression of CXCR5 (Fig. 5 E), demonstrating that specific Ag was required for B cell activation. Although some NP-specific B cells would be expected to bind soluble NP-33D1 directly, the lack of significant B cell activation in mice receiving nontargeting NP-rat2b isotype control indicates that Ag uptake by DCIR2+ DCs was required for B cell activation. Consistent with this, analysis of splenocytes from B6 mice injected 30 min previously with Fluor-conjugated NP-33D1 showed that CD8α− DC-associated lectin 2 (DCAL2)− DCs (which are DCIR2+; Kasahara and Clark, 2012), and not B cells or other DC subsets, were the only cells that bound the Ag, indicating that DCIR2+ DCs are the first cells to acquire Ag upon i.v. injection (Fig. 5 F).

We also analyzed B cell activation in NP-DEC205–immunized animals 24 h p.i. As seen with Ag-specific B cells from mice immunized with NP-33D1 or NP-rat2b, NP binding was likewise significantly decreased on Ag-specific B cells from NP-DC205–immunized mice, indicating they had seen Ag (unpublished data). Ag-specific B cells from NP-DEC205–immunized animals also up-regulated CD86 and MHCII, but the increases in their expression were never as high as those seen in mice that received NP-33D1 (Fig. 5 G). In contrast to animals that received NP-33D1, however, we observed no significant increase in CD69 or CCR7 expression, or down-regulation of CXCR5 on Ag-specific B cells from DEC205-immunized mice. Thus, Ag delivery to DEC205+ DCs induced modest increases
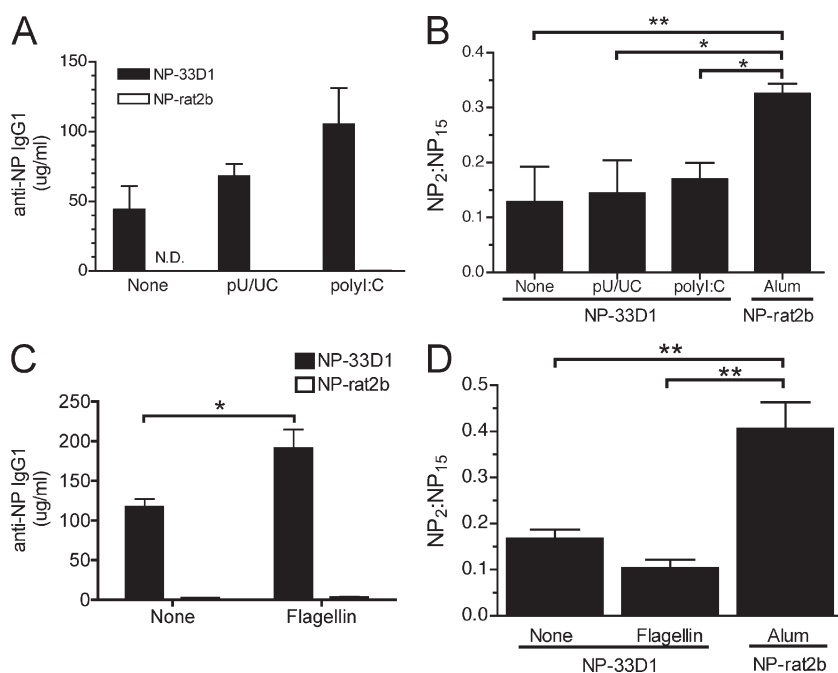

Figure 4. **Agonists for TLR3, TLR5, or RIG-I do not increase affinity maturation of serum Ab after NP-33D1 immunization.** (A) Day 28 anti-NP Ab responses from C57BL/6 mice immunized with NP-33D1 or NP-rat2b with or without 100 µg pU/UC ssRNA or 50 µg polyI:C. Means ± SEM are graphed. (B) Relative affinity ELISA assay showing the ratio of anti-NP IgG quantities that bound NP_2 versus NP_{15} for the groups shown in A. Means ± SEM are graphed. Ab responses in mice immunized with NP-rat2b plus alum are shown as a positive reference for affinity maturation. Data in A and B are representative data from two independent experiments using three to four mice/group. (C and D) C57BL/6 mice were immunized with NP-33D1 with or without 20 µg flagellin and analyzed as A and B. Data are representative of three independent experiments using three mice/group and depict the mean ± SEM. Statistical differences were calculated using two-way ANOVA (A and C) or one-way ANOVA followed by Bonferroni's post-tests (B and D). P-value indicators ** and * refer to $P < 0.01$ and $P < 0.05$, respectively.
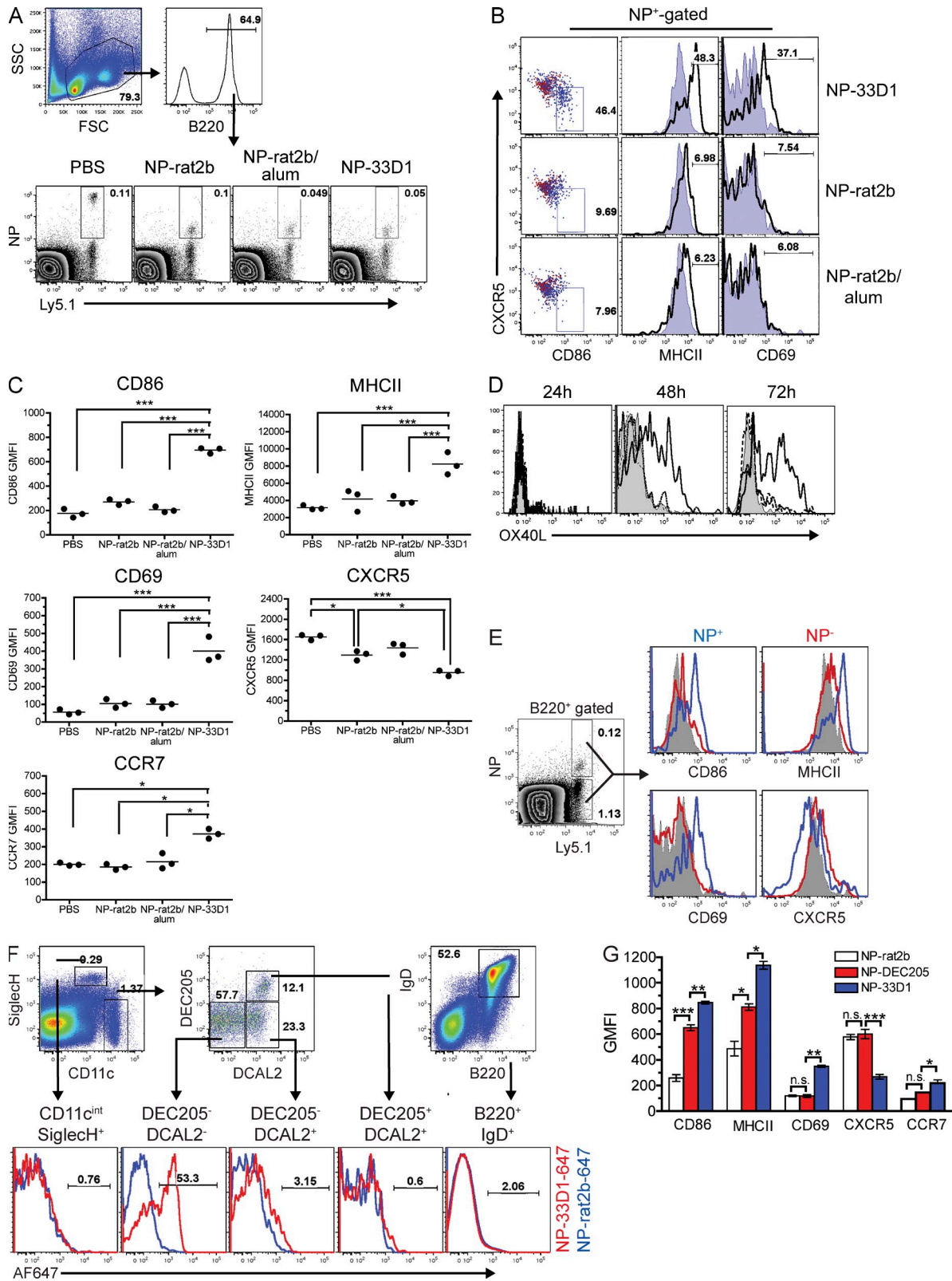
Figure 5. Ag–specific B cells are rapidly activated in vivo after Ag uptake by DCIR2+ DCs. (A) Flow cytometry plots show the gating strategy for identification of adoptively transferred Ly5.1+ NP-binding B1-8hi B cells from the spleens of C57BL/6 recipients immunized as indicated 24 h previously. Numbers denote frequency of gated cells among total B220+ lymphocytes. (B) Expression of CD69, CD86, MHCII, and CXCR5 among NP-binding Ly5.1+ B cells gated in A for immunized mice (blue dots and solid lines) and PBS–injected controls (red dots and shaded histograms). (C) Geometric mean fluorescence intensities (MFIs) are plotted for
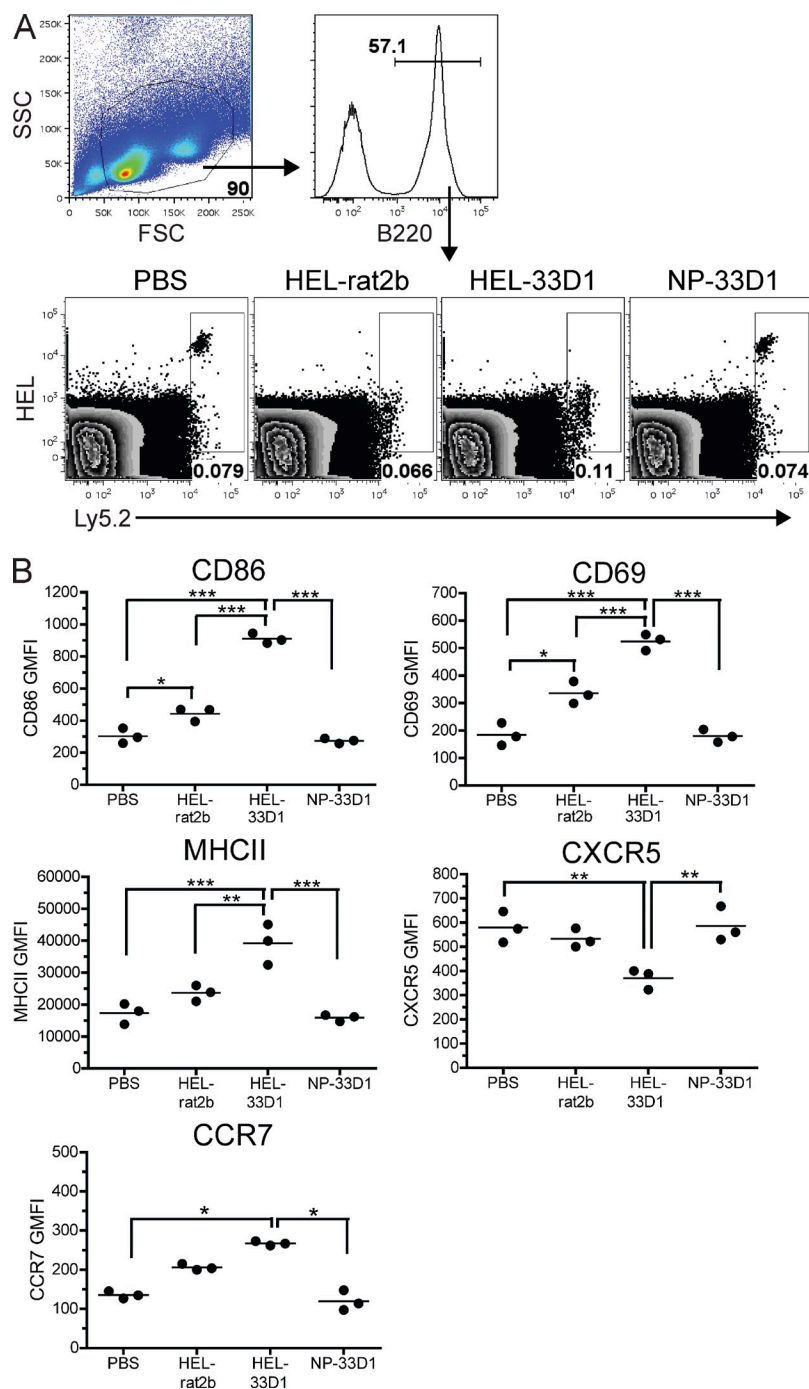
Figure 6. DC–mediated B cell activation requires specific Ag. (A) Flow cytometry plots show gating of adoptively transferred Ly5.2⁺ HEL-binding VDJ9κ5 B cells from the spleens of recipient Ly5.1⁺ congenic C57BL/6 mice immunized as indicated 24 h previously. Numbers denote frequency of gated cells among total B220⁺ lymphocytes. (B) MFIs of the indicated surface marker 24 h p.i. among HEL-binding Ly5.2⁺ B cells gated in A. Each dot represents an individual animal with the mean (horizontal bars) indicated. Data in A and B are representative data from three independent experiments using three mice/group. Statistical differences were calculated using one-way ANOVA analysis followed by Bonferroni's post-tests. P-value indicators ***, **, and * refer to P < 0.001, P < 0.01, and P < 0.05, respectively.

in B cell activation markers but failed to induce changes in expression of receptors that regulate B cell migration.

Ag-specific B cell activation after NP-33D1 immunization was not unique to hapten-specific B cells because adoptively transferred HEL-specific B cells from VDJ9κ5 mice also displayed decreased Ag binding capability (Fig. 6 A) and were similarly activated after injection of HEL-coupled 33D1 (HEL-33D1), but not control rat IgG2b (HEL-rat2b; Fig. 6 B). Furthermore, HEL-specific B cells did not decrease Ag binding or become activated after immunization of VDJ9κ5 recipients with NP-33D1, again indicating the requirement for specific Ag (Fig. 6, A and B). Finally, the observed NP-specific B cell activation in NP-33D1–immunized recipients was not a result of the use of B cells with a high-affinity for Ag because low-affinity NP-specific B cells from B1-8ˡᵒ mice (Shih et al., 2002b) were similarly activated after NP-33D1 immunization (unpublished data).

These results strongly suggested that rapid activation of B cells after Ag uptake by DCIR2 is DC dependent. However, cognate interactions with CD4 T cells can also contribute to B cell activation. To determine whether

the indicated surface molecule among NP-binding Ly5.1⁺ B cells gated in A. Each dot represents an individual animal with the mean (horizontal bars) indicated. Data shown in A–C are representative data from more than four independent experiments using three to four mice/group. (D) Up-regulation of OX40L expression over time among transferred Ly5.1⁺ NP-binding B cells from C57BL/6 recipients that received NP-33D1 (solid line), NP-rat2b (dotted line), NP-rat2b plus alum (dashed line), or PBS-injected controls (shaded). Data are representative of two independent experiments using three mice/group. (E) Expression of the indicated activation marker is graphed for gated NP⁺ (blue line) and NP-negative (red line) populations from mice in A immunized with NP-33D1. Shaded histograms depict NP-binding B cells from a PBS-injected control for reference. (F) The top shows gating strategy for analysis of DC subsets and B cells. The bottom shows AF647 fluorescence among the indicated population 30 min after injection of 10 µg NP-33D1 (red line) or NP-rat2b (blue line) conjugated to Alexa Fluor 647. Data are representative of two independent experiments using two to three mice/group. (G) MFIs of the indicated surface marker are plotted for transferred NP-specific B cells (gated as in A) obtained from C57BL/6 recipients immunized with 10 µg NP-rat2b, NP-DEC205, or NP-33D1. The mean ± SEM from a representative experiment of three independent experiments using three to four mice/group is shown. P-value indicators ***, **, and * refer to P < 0.001, P < 0.01, and P < 0.05, respectively.
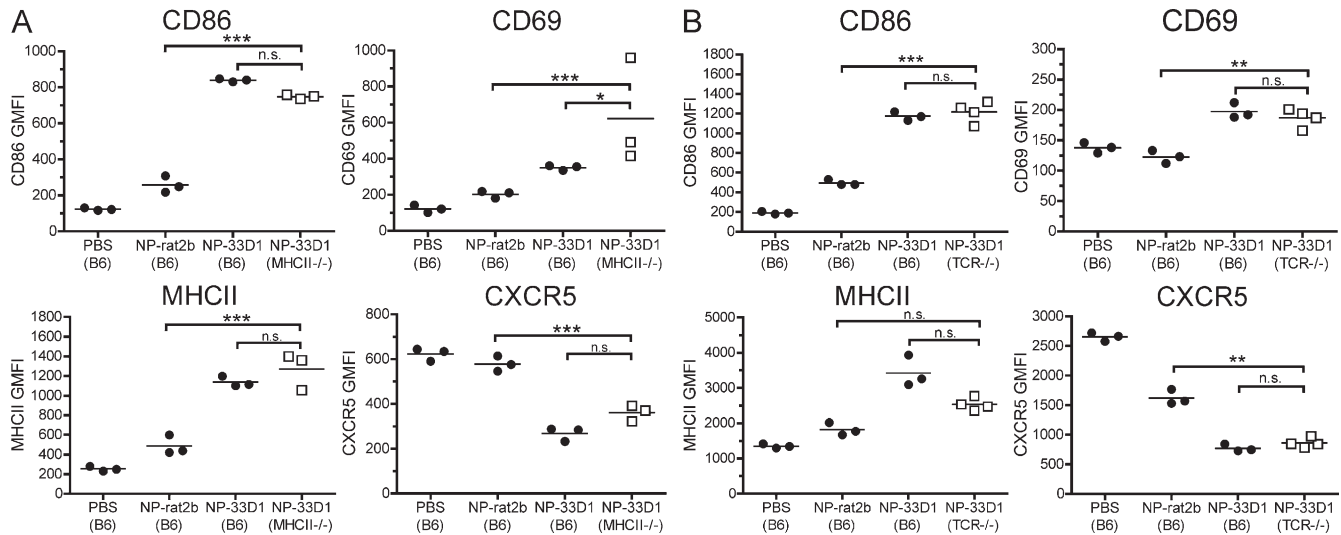
Figure 7. DC-mediated B cell activation is TI. (A and B) MFIs of the indicated surface marker are plotted for NP-binding B cells (gated as in Fig. 5 A) obtained from C57BL/6 and MHCII-deficient (A) or TCR-β/δ–deficient (B) hosts 24 h after immunization with NP-33D1 or NP-rat2b as indicated. Each dot represents an individual animal with the mean (horizontal bars) indicated. Data in A and B are representative data from two independent experiments each using three to four mice/group. Data were analyzed by one-way ANOVA analyses followed by Bonferroni's post-tests. P-value indicators ***, **, and * refer to P < 0.001, P < 0.01, and P < 0.05, respectively. n.s. = not significant.

T cells were required for early B cell activation after Ag delivery to DCIR2⁺ DCs, we immunized B6, MHCII⁻/⁻, and TCR-β/δ⁻/⁻ B1-8ʰⁱ recipient mice with NP-33D1 and assessed B cell activation. NP-specific B cells from both MHCII–deficient (Fig. 7 A) and T cell–deficient (Fig. 7 B) animals showed equal or greater activation after NP-33D1 immunization compared with NP-specific B cells from B6 control recipients. Collectively, these data show that Ag uptake via DCIR2 in vivo leads to rapid TI B cell activation that requires presentation of specific Ag to B cells by DCIR2⁺ DCs.

Ag–specific B cells rapidly accumulate in bridging channels after Ag uptake by DCIR2⁺ DCs

DCIR2⁺ DCs are highly enriched within MZ–associated bridging channels, where there is a convergence of red pulp together with B and T cell regions (Fig. 8 A). As early as 1 d after immunization of mice with NP-33D1, Ag-specific B cells showed decreased CXCR5 expression (Fig. 5, B and C) and elevated levels of CCR7 (Fig. 5 C). These chemokine receptors play a critical role in directing B cell migration (Pereira et al., 2010); therefore, we determined the location of Ag-specific B cells after Ag delivery to DCIR2⁺ or DEC205⁺ DCs. Confocal analysis of frozen spleen sections revealed a striking accumulation of NP-binding B cells at the apical poles of B cell follicles 24 h after injection of NP-33D1 (Fig. 8 B). In contrast, in mice that received NP-rat2b or NP-rat2b plus alum (Fig. 8 B), or NP-DEC205 (Fig. 8 C), NP-specific B cells were rare and confined largely to B cell follicles. In NP-33D1–immunized animals, many NP-specific B cells were in close association with DCIR2⁺ DCs in bridging channels 24 h

p.i. (Fig. 8 D) and were often positioned toward the border with T cell zones (Fig. 8 E). Similar results were obtained when HEL–specific B cell migration was assessed in recipients of VDJ9κ5 B cells 24 h after HEL-33D1 administration (Fig. 8 F). Specific Ag was required for B cell accumulation in bridging channels because HEL–specific B cells failed to migrate after administration of NP-33D1 (Fig. 8 F). On day 2 p.i., NP-binding B cells had begun to disassociate from the bridging channels and many were found migrating along T-B borders (Fig. 8 G), as expected for a TD immune response. By day 3 p.i., nearly all NP-binding B cells were found within the T cell zone or along T-B borders (Fig. 8 G). On day 4 p.i., we observed NP-binding B cells once again in extrafollicular bridging channels, with some cells found outside these regions in the red pulp (Fig. 8, G and H). The small number of NP-binding B cells detectable in the red pulp on day 4 agrees with the earliest time point when NP-specific AFCs were detected by ELISPOT after NP-33D1 immunization (Fig. 1 E). These results reveal a process that begins with B cell activation in DC–rich bridging channels before their migration to T cell zones where they could interact with CD4 T cells, followed by migration once again through the bridging channels, presumably en route toward the red pulp.

B cells primed by DCIR2 DCs drive naive CD4 T cell proliferation in vitro

Previous studies have shown that DCIR2 DCs are efficient APCs for induction of CD4 T cell proliferation after Ag uptake by DCIR2 (Dudziak et al., 2007). Our finding that B cells are highly activated (Fig. 5) and migrate to T cell zones (Fig. 8) after administration of NP-33D1 suggested that they
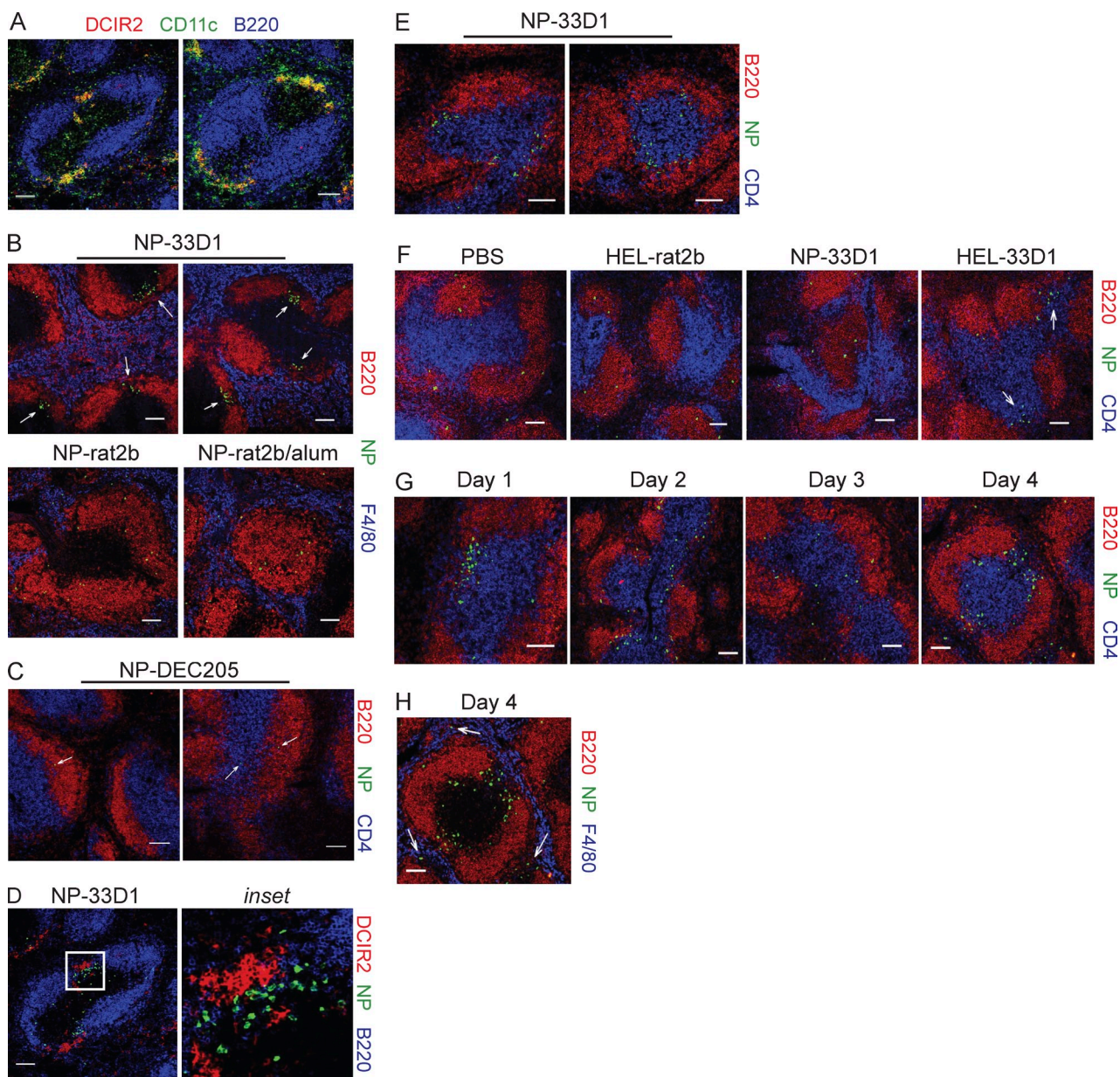
Figure 8. NP–specific B cells rapidly accumulate in MZ bridging channels after Ag delivery to DCIR2+ DCs. 6–8-μm sections were prepared from frozen spleens of B1-8hi or VDJ9κ5 recipient C57BL/6 mice immunized 1–4 d earlier with NP-rat2b, NP-rat2b plus alum, NP-DEC205, or NP-33D1 and stained to determine the location of Ag-specific B cells and/or DCIR2+ DCs. (A) Two examples showing colocalization of DCIR2+ (red) and CD11c+ (green) cells in bridging channels between B cell follicles (blue) in B1-8hi recipients immunized 24 h previously with NP-33D1. (B) NP-binding B cells (green) accumulate at apical poles (arrows) of B220+ B cell follicles (red) 24 h after administration of NP-33D1 (two examples, top row), but not NP-rat2b or NP-rat2b plus alum (bottom row). (C) Two examples indicating NP-binding B cells (green, arrows) do not localize to T cell zones (blue) or bridging channels 24 h p.i. with NP-DEC205. (D) NP-binding B cells (green) found in extrafollicular bridging channels are in close association with DCIR2+ DCs (red) 24 h after immunization with NP-33D1. (E) Two examples showing NP-binding B cells (green) are oriented toward T cell zones (blue) 24 h p.i. with NP-33D1. Data in A–E are representative data from three independent experiments from which more than five sections were analyzed from two or more animals from each group. (F) HEL-binding B cells (green) accumulate in bridging channels (arrows) 24 h p.i. with HEL-33D1, but not NP-33D1. Data in F are representative of two independent experiments from which more than five sections from two animals from each group were analyzed. (G) NP-binding B cells (green) migrate from bridging channels (day 1) to CD4 T cell areas (blue; days 2 and 3) before relocating on day 4 to bridging channels (G) and F4/80+ red pulp (blue; H) after immunization with NP-33D1 (arrows indicate extrafollicular NP-binding B cells). Data for days 2–4 are representative of more than five sections analyzed from two animals for each time point from a single experiment. Bars, 100 μm.

may be able to present Ag to T cells. Therefore, we compared the ability of Ag-specific and polyclonal B cells, as well as DCIR2+ DCs recovered from immunized mice, to induce

OVA-specific CD4 T cell proliferation in vitro after administration of NP-33D1 or NP-rat2b conjugated to OVA (NP-OVA-33D1 and NP-OVA-rat2b, respectively; Fig. 9 A).
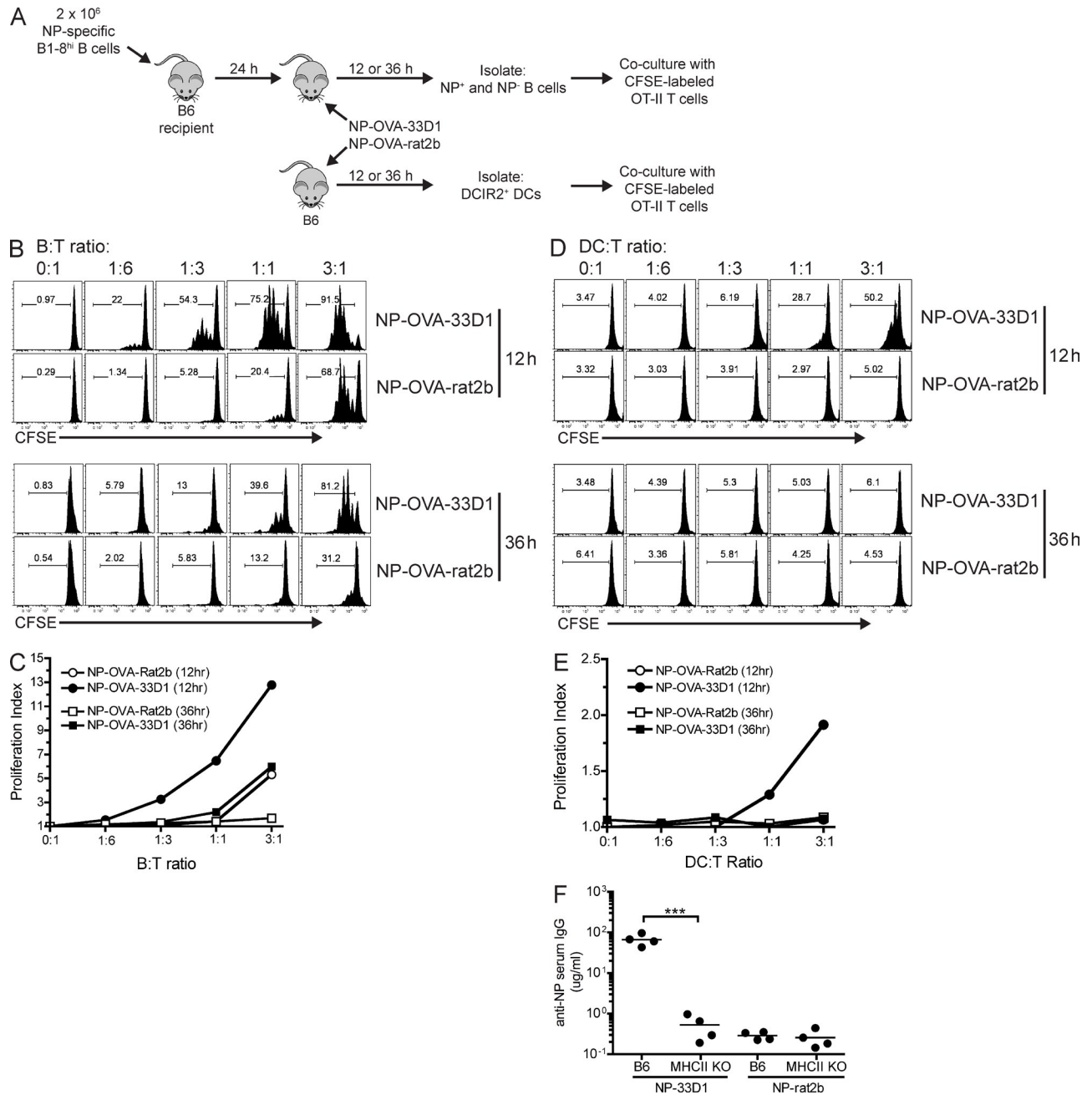
Figure 9. **Ag–specific B cells primed by DCIR2+ DCs are highly efficient APCs for CD4 T cell proliferation.** (A) Schematic showing experimental design. (B) Histograms show dilution of CFSE among gated CD4+Va2+ OT-II T cells after 72 h in culture with NP-specific B cells from spleens of B1-8hi recipient C57BL/6 mice immunized 12 or 36 h previously with NP-33D1 or NP-rat2b. (C) Proliferation indices generated from the data in B are shown. (D) Same as in B, except sorted DCIR2+ DCs from spleens of immunized C57BL/6 mice were used as APCs. (E) Proliferation indices generated from the data in D are shown. Proliferation index is defined as total CFSE fluorescence of the negative control (APC/T cell ratio of 0:1) divided by total CFSE fluorescence of indicated samples. A representative experiment of two independent experiments for each time point is shown for both B and D. (F) Day 12 anti-NP IgG Ab responses in MHCII-deficient and C57BL/6 recipients of OT-II CD4 T cells and B1-8hi B cells after immunization with NP-OVA–33D1 or NP-OVA–rat2b is shown. Each dot represents an individual animal with the mean (horizontal bars) indicated. A representative experiment of two independent experiments using four to five mice/group is shown. P-value indicator *** refers to P < 0.001.

NP-specific B cells recovered from mice 12 or 36 h after immunization with NP-OVA–33D1 induced robust Ag-specific CD4 T cell proliferation compared with NP-specific B cells from mice that received NP-OVA–rat2b (Fig. 9 B).

Although the latter group induced some CD4 proliferation at the highest B/T cell ratio (3:1), this was much reduced compared with NP-OVA–33D1 at both 12 and 36 h (Fig. 9 C). Polyclonal B cells from either group failed to induce CD4
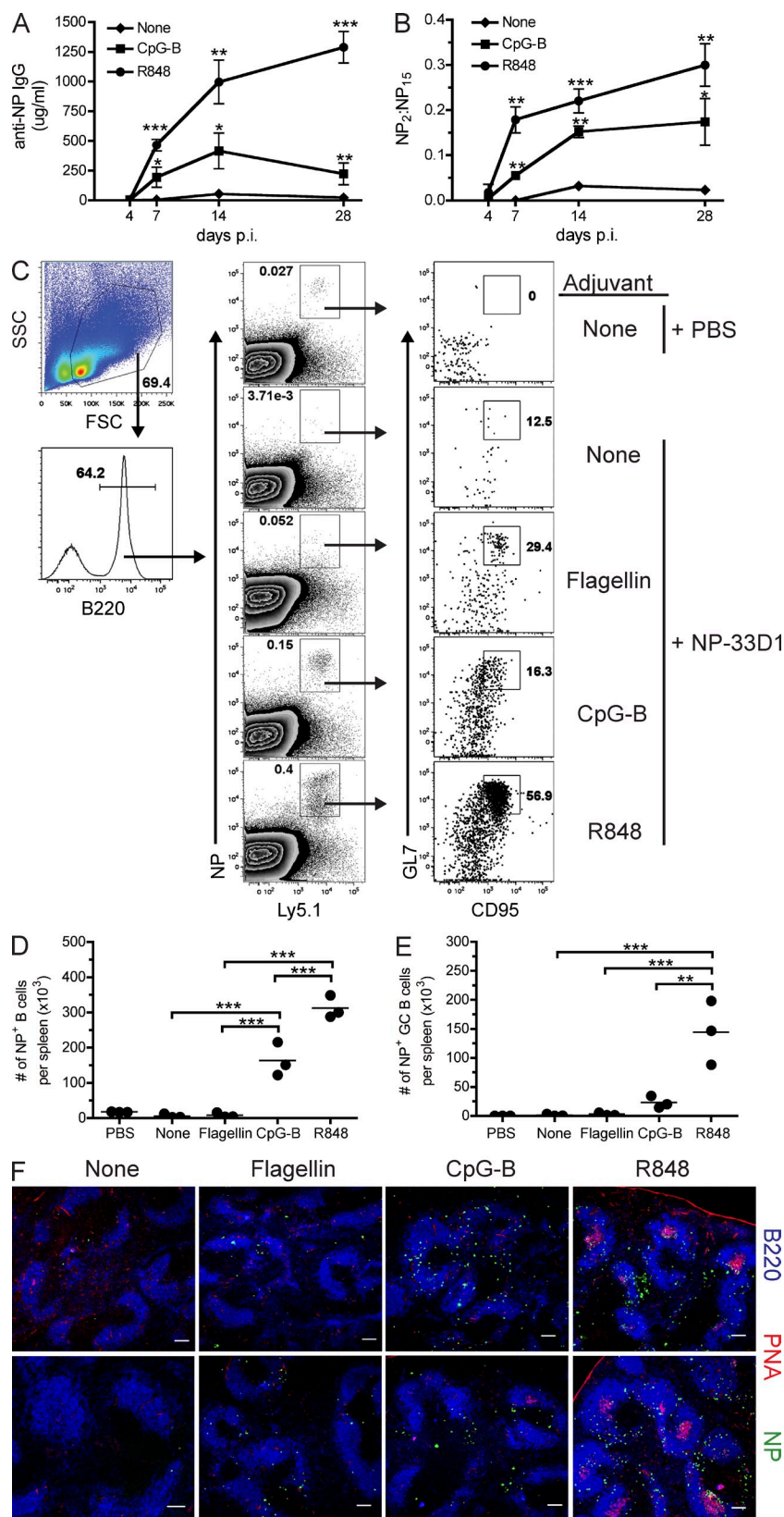
Figure 10. TLR7 and TLR9 agonists promote increased Ab responses, GC formation, and affinity maturation of serum Ab. (A) Kinetics of anti-NP IgG Ab responses in C57BL/6 mice that received NP-33D1 alone or together with 20 µg R848 or 50 µg CpG-B. (B) Kinetics of affinity maturation among total anti-NP IgG serum Ab from the animals in A. Statistical values comparing each group with NP-33D1–only control were generated using an unpaired Student's *t* test. Data in A and B depict a representative experiment of two independent experiments using three mice/group. Means ± SEM are graphed. (C) C57BL/6 recipients of B1-8^{hi} B cells were immunized as indicated and analyzed on day 7 p.i. Flow cytometry plots show gating strategy (left column) and frequency of NP-binding B cells (middle column) among total B220^{+} B cells. Right column shows expression of GL7 and Fas among gated NP-binding B cells. Numbers indicate frequency of GC B cells among total NP-binding B cells. Total numbers per spleen of NP-binding B cells (D) and NP-binding GC B cells (E) are plotted for the mice in C. Each dot represents an individual animal with the mean (horizontal bars) indicated. Data in C–E are representative of two independent experiments using three to four mice/group. Statistical values were generated using one-way ANOVA analyses followed by Bonferroni's post-tests. (F) Immunofluorescence showing GC formation 7 d p.i. in spleen sections derived from mice immunized as in C and stained with B220 (blue), PNA (red), and NP (green). Two examples from each immunization are shown (top and bottom rows). Bars, 100 µm. Data are representative of more than six sections per mouse taken from two mice per condition. P-value indicators ***, **, and * refer to $P < 0.001$, $P < 0.01$, and $P < 0.05$, respectively.

CD4 T cell proliferation (e.g., proliferation index of 12.8 for B cells vs. 1.9 for DCs at 3:1 ratio) and were unable to do so 36 h p.i. (Fig. 9, D and E). The sorted DCIR2^{+} DCs were capable of Ag presentation at both 12 and 36 h because peptide-pulsed DCIR2^{+} DCs induced robust OT-II T cell proliferation in co-cultures performed in parallel (unpublished data). Analysis of DC viability during the 3-d culture revealed no differences in DC survival from mice injected 12 h previously with NP-OVA-33D1 or NP-OVA-rat2b, suggesting that DCIR2 cross-linking by 33D1 mAb does not induce apoptosis (unpublished data).

The striking difference in the ability of Ag-specific B cells and DCIR2^{+} DCs to induce CD4 T cell proliferation in vitro

T cell proliferation (unpublished data). Surprisingly, compared with NP-specific B cells, DCIR2^{+} DCs isolated from animals immunized 12 h earlier induced relatively weak suggested that DC-mediated Ag presentation to CD4 T cells may be dispensable for Ab responses induced by NP-33D1 immunization. To test this, we immunized C57BL/6 and

MHCII-deficient mice that received both Ag-specific OT-II T cells and B1-8^{hi} B cells with NP-OVA-33D1 or NP-OVA-rat2b. MHCII-deficient recipients were unable to mount a significant Ab response after NP-OVA-33D1 immunization compared with C57BL/6 recipients (Fig. 9 F). These results show that DCIR2-primed B cells are highly efficient APCs for driving CD4 T cell proliferation and that cognate DC–T cell interaction is required for DCIR2-induced Ab responses.

TLR7 and TLR9 agonists significantly enhance Ab responses and affinity maturation

The TLR5 agonist flagellin can activate DCs and promote T$_H$2-driven Ab responses in vivo (Didierlaurent et al., 2004; Letran et al., 2011), yet it failed to promote affinity maturation when administered in conjunction with NP-33D1 (Fig. 4 D). This result, together with those showing that B cells primed by DCIR2$^+$ DCs are highly efficient APCs, prompted us to determine whether inclusion of agonists for TLRs highly expressed in B cells would induce GC formation and affinity-matured Ab in mice immunized with NP-33D1. TLR7 and TLR9, unlike TLR3, TLR5, and RIG-I, are expressed at high levels in mouse B cells (Gururajan et al., 2007). Immunization of mice with NP-33D1, together with agonists for TLR7 (R848) or TLR9 (CpG-B), showed that inclusion of either agonist significantly increased total anti-NP IgG production (Fig. 10 A); however, R848 had the greatest impact, resulting in >50-fold more anti-NP Ab at day 28 p.i. compared with NP-33D1 alone. Immunization of mice with NP-rat2b plus TLR7 or TLR9 agonists failed to generate anti-NP Abs, demonstrating that TLR-enhanced Ab production was dependent on DC-mediated B cell activation (unpublished data).

In contrast to NP-33D1 alone or in conjunction with flagellin (Fig. 4 D), both TLR7 and TLR9 agonists significantly increased high-affinity anti-NP Ab production (Fig. 10 B), suggesting that these agonists also induced GC formation. Using the B1-8 adoptive transfer system, we found that agonists for TLR7 and TLR9, but not TLR5, each enhanced the frequency and number of NP-specific B cells (Fig. 10, C and D). Interestingly, R848 (TLR7 agonist) was the only agonist to significantly enhance the expansion of GL7$^+$Fas$^+$ GC B cells (Fig. 10, C and E) in B1-8 recipients. These results were confirmed by conventional histology which showed significant accumulation of NP-specific B cells in the red pulp in mice that received CpG-B or R848, demonstrating that these adjuvants induced a strong extrafollicular response (Fig. 10 F). Importantly, only mice that received R848 together with NP-33D1 contained numerous PNA$^+$ GCs, which were sparse in mice that received CpG-B and absent in mice that received flagellin (Fig. 10 F). These results demonstrate that in the context of Ag delivery to DCIR2$^+$ DCs, select secondary stimuli is required to alter the B cell differentiation program toward GC formation and production of high-affinity Ab.

DISCUSSION

In this study, we focused on B cell responses after Ag uptake by two distinct subsets of splenic DCs in mice. We show that Ag delivery to the CLR DCIR2 expressed on MZ-associated CD8α$^-$ DCs generates robust TD IgG1-restricted Ab responses without generating detectable levels of IgM. In contrast, Ag uptake via DEC205 found on CD8α$^+$ DCs induced very weak Ag-specific Ab responses. We found that DCIR2-induced Ab responses correlated with the ability of DCIR2$^+$ DCs to mediate rapid B cell activation and migration in vivo, which resulted in the generation of Ag-specific B cells highly proficient at driving naive CD4 T cell proliferation. The IgG1-restricted TD Ab responses induced by DCIR2$^+$ DCs differed markedly from the rapid TI IgM-restricted responses that are seen when Ag enters lymphoid tissue associated with CD11c^{lo} blood-derived DCs (Balázs et al., 2002). These results show that the context in which Ag enters lymphoid tissues has a profound influence on the ensuing Ab response and suggest that, in addition to the selective activation of T cells by DC subsets, a similar paradigm exists regarding DC subpopulations and their ability to activate B cells and induce humoral immune responses.

The manner in which B cells acquire their Ag, and how this event influences the humoral response, is a critical yet poorly understood aspect of B cell biology. After subcutaneous injection of Ag-loaded DCs, Qi et al. (2006) directly visualized DC-mediated activation of Ag-specific B cells via Ag transfer in regions proximal to high endothelial venules within lymph nodes. Although these studies provided direct evidence for DC–B cell interactions in vivo, the contribution of individual DC subsets to B cell activation and subsequent Ab responses was not investigated. Our approach of delivering Ag directly to DC subsets in vivo revealed a remarkable contrast in the ability of DCIR2$^+$ versus DEC205$^+$ DCs to activate B cells and induce Ab production after Ag uptake in situ. It is unclear from our studies whether B cells obtain all their Ag directly from DCIR2 DCs or whether they collect further free circulating Ag after becoming activated. NP-specific B cells from mice injected with nontargeting NP-rat2b isotype control take up Ag in vivo, as indicated by decreased Ag binding in vitro (Fig. 5 A). However, Ag presentation by DCIR2$^+$ DCs to B cells was required for activation because administration of nontargeting NP-rat2b, which would be expected to remain in circulation as long as NP-33D1, failed to induce either B cell activation or plasma cell differentiation.

Although other groups have noted the inability of Ag uptake via DEC205 to induce robust Ab responses in the absence of adjuvants (Lahoud et al., 2009, 2011; White et al., 2010), our analysis is the first to correlate DC-induced B cell activation and migration with the ability of a DC subset to induce humoral immune responses. Ag delivery to DEC205$^+$ DCs resulted in increased CD86 and MHCII expression on Ag-specific B cells (which were decreased compared with those induced by DCIR2$^+$ DCs), yet DEC205$^+$ DCs failed to down-regulate CXCR5 expression or up-regulate CCR7 levels on Ag-specific B cells. These changes in chemokine

receptor expression are critical for B cell migration to the T–B border, a required step for T–B collaboration during TD humoral immune responses (McHeyzer-Williams et al., 2003; Pereira et al., 2010). Furthermore, DEC205+ DCs failed to up-regulate CD69 expression on Ag-specific B cells. In addition to its utility as an early marker of lymphocyte activation, CD69 is a negative regulator of $S1P_1$ (sphingosine-1-phosphate receptor 1) activity (Shiow et al., 2006), which is required for B cell egress from lymphoid tissues (Schwab and Cyster, 2007). Thus, despite increases in markers which facilitate T–B cognate interactions, Ag-specific B cells from DEC205-immunized animals failed to alter expression of critical trafficking receptors and their regulators, and hence were unable to properly position themselves for collaboration with CD4 T cells. This was confirmed by our confocal analysis of spleen sections 24 h p.i. that show Ag-specific B cells in DEC205-immunized mice were sparse and found within B cell follicles or red pulp but not the T cell zones where DEC205+ DCs are located (Fig. 8 C). In contrast, Ag-specific B cells from DCIR2-immunized mice showed significant accumulation in MZ-associated bridging channels that are densely populated by DCIR2+ DCs (Fig. 8, A and B; Czeloth et al., 2007; Dudziak et al., 2007). These results provide a mechanistic explanation for the observations that Ag delivery to some DC subsets can induce robust Ab responses, whereas Ag delivery to other DC subsets does not (Corbett et al., 2005; Lahoud et al., 2009, 2011; White et al., 2010).

Why are DCIR2+ DCs able to effect these changes on B cells? Several possibilities may explain the superior ability of DCIR2+ DCs to efficiently activate Ag-specific B cells in vivo. First, their position within the extrafollicular bridging channels is ideally suited to enhance encounters with rare Ag-specific B cells immigrating from the circulation. This is supported by our observation that many more Ag-specific B cells are detected in individual spleen sections of mice 24 h after NP-33D1 administration compared with mice that received PBS or NP-rat2b controls (Fig. 8 B). This is unlikely a result of B cell division at such an early time point, suggesting that B cell accumulation in bridging channels is due in part to capture of B cells exiting circulation. In contrast, DEC205+ DCs are found primarily in the PALS, a region which does not receive much lymphocyte traffic, and therefore encounter of Ag-specific B cells with Ag-bearing DEC205+ DCs is likely to be much more infrequent. Second, DCIR2+ DCs may secrete one or more chemokines that attract B cells from the follicles. Although cross-linking DCIR2 by the 33D1 mAb does not induce up-regulation of classical DC activation markers, the secretion of chemokines has not been investigated. Consistent with this notion, we were unable to find Ag-specific B cells in the follicles of DCIR2-immunized mice. Third, the receptor DCIR2 likely has a role in this process. It is unclear at present whether Ag internalized by DCIR2 is returned to the surface in its native form, similar to Ag internalized by FcγRIIb (Bergtold et al., 2005). Ag internalization by DCIR2 has been noted to occur more slowly than DEC205-mediated internalization

(Dudziak et al., 2007). A slower rate of internalization could result in prolonged display of surface Ag and potentially allow for more sustained BCR engagement, leading to both greater B cell activation and increased acquisition of Ag.

Similar to DCIR2, Ag delivery to the CLR Clec9a also induces robust Ab responses in the absence of adjuvant (Caminschi et al., 2008). Unlike DCIR2, however, Clec9a is highly expressed on mature CD8α+DEC205+ DCs, CD8α−CD24hiMHCII+/− precursors of CD8α+ DCs, and CD11cint pDCs (Caminschi et al., 2012). In this case, it was shown that the ability of Clec9a+ DCs and their precursors to induce CD4 T cell proliferation is the correlative marker for Ab production after Ag delivery to Clec9a. In contrast, we found that CD4 T cell proliferation induced by DCIR2+ DCs in vitro was less efficient than that induced by Ag-specific B cells after immunization with NP-OVA-33D1 (Fig. 9). Dudziak et al. (2007) have reported that DCIR2+ DCs induce robust proliferation of CD4 T cells. Although a direct comparison of the in vitro data are not possible because of the use of different assays (CFSE versus thymidine incorporation), we did observe robust OT-II CD4 T cell proliferation in vivo in C57BL/6 recipients after immunization with OVA-33D1 (unpublished data), similar to the results of Dudziak et al. (2007). This observation further strengthens the conclusion that the correlative marker of humoral immune responses after Ag delivery to DCIR2+ DCs is the ability of the DC to prime B cells to become highly effective APCs for CD4 T cells. Overall, it appears that individual DC subsets may use different mechanisms to drive Ab production.

Because immunization with NP-33D1 exclusively yields low-affinity extrafollicular Ab responses, this approach provided a unique opportunity to investigate signals that influence GC versus extrafollicular AFC differentiation. BCR affinity for Ag is a critical factor that influences B cell differentiation (Shih et al., 2002a; Paus et al., 2006); however, other factors or cell types may be involved (Odegard et al., 2008). GC B cell differentiation requires interaction with CD4 T_{FH} cells (Crotty, 2011). Most models of T_{FH} differentiation suggest DCs are required for their development, which is sustained via subsequent interactions with Ag-specific B cells (Haynes et al., 2007; Crotty et al., 2010; Deenick et al., 2010). Surprisingly, agonists for pattern recognition receptors that can activate DCs and/or promote type I IFN (Didierlaurent et al., 2004; Saito et al., 2008; Longhi et al., 2009) failed to promote GC B cell differentiation or affinity maturation after NP-33D1 immunization (Fig. 4). Instead, inclusion of TLR7 agonist together with NP-33D1 immunization markedly enhanced total Ab responses and supported GC differentiation and high-affinity Ab production (Fig. 10). The mechanism underlying TLR7-induced GC differentiation likely involves several factors. Stimulation via TLR7 elicits type I IFN production from pDCs (Akira et al., 2006), which can act directly on B cells and CD4 T cells to promote CSR and T_{FH} development, respectively (Braun et al., 2002; Le Bon et al., 2006; Cucak et al., 2009). However, polyI:C and pU/UC also induce type I IFN, yet these agonists failed

to induce high–affinity Ab production (Fig. 4), suggesting that induction of type I IFN is not the sole mechanism by which TLR7 and TLR9 mediate affinity maturation. Alternatively, enhanced B cell–driven T_{FH} differentiation may play a role. Further experiments are needed to discriminate among these possibilities.

By comparing the early response of Ag–specific B cells after Ag delivery to two distinct DC subsets, we provide new insight into the events that are required for DC-induced Ab responses. Our results suggest a model whereby Ag-bearing MZ-associated DCs prime B cells to become efficient APCs for CD4 T cells, a critical event which drives the TD humoral response. This is supported by our findings that agonists for pattern recognition receptors highly expressed in B cells, but not DCs, greatly enhanced both high- and low-affinity Ab production. These results further our understanding of the cellular interactions and molecular signals that govern B cell activation and differentiation, which is critical for the rational design of vaccines aimed at generating protective Ab responses.

MATERIALS AND METHODS

Mice. C57BL/6 mice were bred and maintained by our laboratory or alternatively purchased from The Jackson Laboratory. BALB/c mice, mice deficient in TCR-β/δ or CD40, and CD11cDTR/GFP mice on the C57BL/6 background were purchased from The Jackson Laboratory. Depletion of CD11c$^+$ cells was achieved by injecting CD11cDTR/GFP mice i.p. with 100 ng diphtheria toxin (Sigma-Aldrich) 24 h before immunization, which resulted in depletion of >90% GFP$^+$ CD11c$^+$ DCs (unpublished data). Mice deficient in MHC class II (provided by P. Fink, University of Washington, Seattle, WA), CD40, FcεR γ-chain, TCR-β/δ, CD28 (provided by J. Green, Washington University, St. Louis, MO), and OX40L (provided by A. Sharpe, Harvard University, Cambridge, MA) were backcrossed to C57BL/6 for 12 generations. IL-4–deficient mice (provided by S. Ziegler, Benaroya Research Institute, Seattle, WA) were backcrossed to BALB/c for 10 generations. Mice deficient in the FcεR γ-chain were purchased from Taconic. All strains with gene-targeted deletions were maintained via homozygous breeding. Wild-type mice for controls were C57BL/6, obtained through in-house breeding or purchased from The Jackson Laboratory. OT-II mice (provided by K. Elkon, University of Washington), B1-8^{hi} and B1-8^{lo} mice (both provided by M. Nussenzweig, Rockefeller University, New York, NY), and VDJ9κ5 transgenic mice (provided by J. Cyster, University of California, San Francisco, San Francisco, CA) were backcrossed to C57BL/6 for seven or more generations. All mice used were between 8 and 15 wk of age and maintained under specific pathogen-free conditions. All animal procedures were approved by the Institute for Animal Care and Use Committee at the University of Washington.

Reagents, immunogens, and adjuvants. Rat IgG2b mAbs against DCIR2 (clone 33D1) or rat IgG2b isotype control (clone EB149-10H5, derived from KLH-immunized rats; both from eBioscience) were conjugated to the succinimide ester of NP (Biosearch Technologies) as previously described (Goins et al., 2010). Final NP conjugation ratios ranged from NP$_4$ to NP$_8$ as determined by spectrophotometry, which showed no significant difference in binding to NP-specific B1-8 B cells upon titration as determined by flow cytometry. HEL and chicken OVA (both from Sigma-Aldrich) were conjugated to mAbs as previously described (Weir et al., 1986). Alum-precipitated Ags were prepared with Inject (Thermo Fisher Scientific) according to the manufacturer's instructions. R848 and flagellin from *Bacillus subtilis* (both from InvivoGen) and CpG-B ODN 1226 (Invitrogen) were resuspended in endotoxin-free PBS or water, respectively, and stored at −20°C until use. pU/UC single-stranded (ss) RNA was generated in vitro using the T7 MEGAshortscript RNA synthesis kit (Ambion) as previously described

(Saito et al., 2008). Final reaction products were extracted with TRIzol, extensively washed, resuspended in endotoxin-free water, and stored at −20°C until use. HEL was conjugated to Alexa Fluor 647 using the microscale protein labeling kit according to manufacturer's instructions (Invitrogen).

Immunizations and adoptive transfers. Ag-coupled mAbs were diluted in sterile PBS and administered via tail vein injection i.v. Immunizations consisted of 10 µg mAb, except for experiments in Fig. 1. When used, agonists were admixed with the immunogen and administered i.v. For adoptive transfer experiments, splenic B cells from B1-8^{hi}, B1-8^{lo}, or VDJ9κ5 mice were negatively selected via magnetic enrichment (EasySep B cell enrichment kit; STEMCELL Technologies) and labeled with the proper Fluor-conjugated Ag and anti-B220 to determine the frequency of Ag-specific B cells by flow cytometry. 1–2 × 10^6 (Figs. 5–8) or 2 × 10^5 (Fig. 9) Ag-binding B cells were transferred to B6 or B6.Ly5.1 recipients (as appropriate) 18–24 h before immunization. For OT–II transfers, CD4 T cells were enriched using EasySep CD4 T cell enrichment kit (STEMCELL Technologies) and 10^6 Vα2$^+$ CD4$^+$ T cells were transferred 18–24 h before immunization.

Antibodies and flow cytometry. For analysis of splenic B cell activation, RBC-lysed single cell suspensions were stained with mAbs conjugated to FITC, PE, allophycocyanin, eFluor450, allophycocyanin-eFluor780, PE-Cy7, or biotin. Biotin-conjugated mAbs were revealed with streptavidin-conjugated peridinin chlorophyll protein (PerCP)–Cy5.5 (BD). For analysis of B cells, six- or seven-color flow cytometry was performed by staining the cells with combinations of mAbs against B220, Ly5.1, Ly5.2, CD80, CD86, CD69, MHCII, CD40, OX40L, CCR7, GL7, and CD95 (all from eBioscience), and CXCR4 and CXCR5 (from BD), together with either NP-allophycocyanin or HEL–Alexa Fluor 647. To improve staining for both chemokine receptors and Ag binding, splenocytes were preincubated at 37°C for 30 min in RPMI 1640 containing 10% FBS (Thermo Fisher Scientific) before incubation with Fluor- or biotin-conjugated mAbs at 37°C for 30 min. Secondary staining with streptavidin–PerCP-Cy5.5 was performed on ice for 20 min in the dark. Primary staining for CD4 T cell proliferation was performed on ice for 20 min in the dark. Data were collected using LSRII or FACScan flow cytometers (BD) and analyzed with FlowJo software (Tree Star).

Cell sorting. For DC purification, pooled spleens were digested with Liberase IV (Roche), followed by magnetic enrichment of CD11c$^+$ cells (Miltenyi Biotec) according to manufacturer's instructions. Enriched cells were labeled with CD11c-FITC, CD8α-PE, B220-PE-Cy7, NK1.1-PE-Cy7, and DCAL2–Alexa Fluor 647. DCIR2$^+$ DCs were isolated by sorting CD11c$^+$B220$^-$NK1.1$^-$ splenocytes that displayed a CD8α$^-$DCAL2$^-$ phenotype (Kasahara and Clark, 2012). For isolation of NP-specific B cells, splenocytes from pooled spleens were enriched for Ig λ$^+$ B cells by including biotinylated anti-kappa mAb (BD) in the B cell enrichment cocktail provided with the EasySep B cell enrichment kit (STEMCELL Technologies). Enriched cells were labeled with NP-PE, B220-eFluor450, and Ly5.1-allophycocyanin before sorting. All sorting was performed using a FACSAria II cell sorter (BD).

In vitro CFSE proliferation assay. CD4 T cells were enriched from pooled spleens of OVA-specific OT-II mice by negative selection using CD4 T cell enrichment kit according to manufacturer's instructions (EasySep). Resulting cells were labeled with CD4-FITC and Vα2-PE to determine the frequency and absolute number of OVA-specific CD4 T cells. Enriched cells were loaded with 2.5 µM CFSE in PBS at 37°C for 10 min, quenched with RPMI 1640 containing 10% FBS, and washed extensively. 8–10 × 10^4 OVA-specific CD4 T cells were placed into culture at 37°C and 5% CO$_2$ together with titrating numbers of sorted APC populations (see previous section). Co-cultures were incubated for 72 h, harvested, and analyzed for CFSE dilution among CD4$^+$Vα2$^+$ T cells by flow cytometry.

Immunohistochemistry. Spleens from immunized B1-8^{hi} or VDJκ9 recipient mice were embedded in OTC medium and frozen at −80°C. 6–8-µM sections were fixed to glass slides and kept at −80°C until use. Sections were

fixed in ice-cold acetone for 15 min, air dried, and stained at room temperature with NP-PE, B220-eFluor450, CD4–Alexa Fluor 647, CD11c-FITC, DCIR2-biotin, PNA-FITC, or F4/80-biotin (eBioscience) for 90 min in PBST (PBS containing 0.05% Tween-20). For detection of HEL-specific B cells, sections were incubated with 200 ng/ml HEL in PBST, followed by secondary incubation with biotinylated anti-HEL (HyHEL9-biotin) for 60 min at room temperature. Biotinylated reagents were revealed with streptavidin-conjugated Alexa Fluor 555 in PBST for 60 min at room temperature. For DCIR2 staining, anti–DCIR2-biotin was detected with secondary biotinylated anti–rat IgG followed by Cyanine5 TSA amplification (PerkinElmer) according to the manufacturer's instructions. Sections were washed in PBS and mounted in Vectashield HardSet mounting medium (Vector Laboratories). Images were collected on an LSM 510 META confocal microscope (Carl Zeiss) with LSM 510 (v 4.2) software (Carl Zeiss) using 10 or 20× objectives at room temperature. Images were processed using ImageJ (National Institutes of Health) and Photoshop (Adobe) software.

ELISA and ELISPOT assays. ELISA and ELISPOT assays were performed as previously described (Goins et al., 2010).

Statistics. Statistical analyses and data presentation were generated using Prism (GraphPad Software). Statistical tests used are indicated in the figure legends.

REFERENCES

Akira, S., S. Uematsu, and O. Takeuchi. 2006. Pathogen recognition and innate immunity. *Cell.* 124:783–801. http://dx.doi.org/10.1016/j.cell.2006.02.015

Balázs, M., F. Martin, T. Zhou, and J. Kearney. 2002. Blood dendritic cells interact with splenic marginal zone B cells to initiate T-independent immune responses. *Immunity.* 17:341–352. http://dx.doi.org/10.1016/S1074-7613(02)00389-8

Barbalat, R., S.E. Ewald, M.L. Mouchess, and G.M. Barton. 2011. Nucleic acid recognition by the innate immune system. *Annu. Rev. Immunol.* 29:185–214. http://dx.doi.org/10.1146/annurev-immunol-031210-101340

Bergtold, A., D.D. Desai, A. Gavhane, and R. Clynes. 2005. Cell surface recycling of internalized antigen permits dendritic cell priming of B cells. *Immunity.* 23:503–514. http://dx.doi.org/10.1016/j.immuni.2005.09.013

Berney, C., S. Herren, C.A. Power, S. Gordon, L. Martinez-Pomares, and M.H. Kosco-Vilbois. 1999. A member of the dendritic cell family that enters B cell follicles and stimulates primary antibody responses identified by a mannose receptor fusion protein. *J. Exp. Med.* 190:851–860. http://dx.doi.org/10.1084/jem.190.6.851

Braun, D., I. Caramalho, and J. Demengeot. 2002. IFN-alpha/beta enhances BCR-dependent B cell responses. *Int. Immunol.* 14:411–419. http://dx.doi.org/10.1093/intimm/14.4.411

Caminschi, I., A.I. Proietto, F. Ahmet, S. Kitsoulis, J. Shin Teh, J.C. Lo, A. Rizzitelli, L. Wu, D. Vremec, S.L. van Dommelen, et al. 2008. The dendritic cell subtype-restricted C-type lectin Clec9A is a target for vaccine enhancement. *Blood.* 112:3264–3273. http://dx.doi.org/10.1182/blood-2008-05-155176

Caminschi, I., D. Vremec, F. Ahmet, M.H. Lahoud, J.A. Villadangos, K.M. Murphy, W.R. Heath, and K. Shortman. 2012. Antibody responses initiated by Clec9A-bearing dendritic cells in normal and Batf3(-/-) mice. *Mol. Immunol.* 50:9–17. http://dx.doi.org/10.1016/j.molimm.2011.11.008

Carrasco, Y.R., and F.D. Batista. 2006. B cell recognition of membrane-bound antigen: an exquisite way of sensing ligands. *Curr. Opin. Immunol.* 18:286–291. http://dx.doi.org/10.1016/j.coi.2006.03.013

Corbett, A.J., I. Caminschi, B.S. McKenzie, J.L. Brady, M.D. Wright, P.L. Mottram, P.M. Hogarth, A.N. Hodder, Y. Zhan, D.M. Tarlinton, et al. 2005. Antigen delivery via two molecules on the CD8- dendritic cell subset induces humoral immunity in the absence of conventional "danger". *Eur. J. Immunol.* 35:2815–2825. http://dx.doi.org/10.1002/eji.200526100

Craxton, A., D. Magaletti, E.J. Ryan, and E.A. Clark. 2003. Macrophage- and dendritic cell—dependent regulation of human B-cell proliferation requires the TNF family ligand BAFF. *Blood.* 101:4464–4471. http://dx.doi.org/10.1182/blood-2002-10-3123

Crotty, S. 2011. Follicular helper CD4 T cells (TFH). *Annu. Rev. Immunol.* 29:621–663. http://dx.doi.org/10.1146/annurev-immunol-031210-101400

Crotty, S., R.J. Johnston, and S.P. Schoenberger. 2010. Effectors and memories: Bcl-6 and Blimp-1 in T and B lymphocyte differentiation. *Nat. Immunol.* 11:114–120. http://dx.doi.org/10.1038/ni.1837

Cucak, H., U. Yrlid, B. Reizis, U. Kalinke, and B. Johansson-Lindbom. 2009. Type I interferon signaling in dendritic cells stimulates the development of lymph-node-resident T follicular helper cells. *Immunity.* 31:491–501. http://dx.doi.org/10.1016/j.immuni.2009.07.005

Cunningham, A.F., F. Gaspal, K. Serre, E. Mohr, I.R. Henderson, A. Scott-Tucker, S.M. Kenny, M. Khan, K.M. Toellner, P.J. Lane, and I.C. MacLennan. 2007. Salmonella induces a switched antibody response without germinal centers that impedes the extracellular spread of infection. *J. Immunol.* 178:6200–6207.

Czeloth, N., A. Schippers, N. Wagner, W. Müller, B. Küster, G. Bernhardt, and R. Förster. 2007. Sphingosine-1 phosphate signaling regulates positioning of dendritic cells within the spleen. *J. Immunol.* 179:5855–5863.

Deenick, E.K., A. Chan, C.S. Ma, D. Gatto, P.L. Schwartzberg, R. Brink, and S.G. Tangye. 2010. Follicular helper T cell differentiation requires continuous antigen presentation that is independent of unique B cell signaling. *Immunity.* 33:241–253. http://dx.doi.org/10.1016/j.immuni.2010.07.015

Depoil, D., S. Fleire, B.L. Treanor, M. Weber, N.E. Harwood, K.L. Marchbank, V.L. Tybulewicz, and F.D. Batista. 2008. CD19 is essential for B cell activation by promoting B cell receptor-antigen microcluster formation in response to membrane-bound ligand. *Nat. Immunol.* 9:63–72. http://dx.doi.org/10.1038/ni1547

Didierlaurent, A., I. Ferrero, L.A. Otten, B. Dubois, M. Reinhardt, H. Carlsen, R. Blomhoff, S. Akira, J.P. Kraehenbuhl, and J.C. Sirard. 2004. Flagellin promotes myeloid differentiation factor 88-dependent development of Th2-type response. *J. Immunol.* 172:6922–6930.

Dubois, B., and C. Caux. 2005. Critical role of ITIM-bearing FcgammaR on DCs in the capture and presentation of native antigen to B cells. *Immunity.* 23:463–464. http://dx.doi.org/10.1016/j.immuni.2005.10.005

Dubois, B., C. Massacrier, B. Vanbervliet, J. Fayette, F. Brière, J. Banchereau, and C. Caux. 1998. Critical role of IL-12 in dendritic cell-induced differentiation of naive B lymphocytes. *J. Immunol.* 161:2223–2231.

Dudziak, D., A.O. Kamphorst, G.F. Heidkamp, V.R. Buchholz, C. Trumpfheller, S. Yamazaki, C. Cheong, K. Liu, H.W. Lee, C.G. Park, et al. 2007. Differential antigen processing by dendritic cell subsets in vivo. *Science.* 315:107–111. http://dx.doi.org/10.1126/science.1136080

Fayette, J., I. Durand, J.M. Bridon, C. Arpin, B. Dubois, C. Caux, Y.J. Liu, J. Banchereau, and F. Brière. 1998. Dendritic cells enhance the differentiation of naïve B cells into plasma cells in vitro. *Scand. J. Immunol.* 48:563–570. http://dx.doi.org/10.1046/j.1365-3083.1998.00471.x

Flynn, S., K.M. Toellner, C. Raykundalia, M. Goodall, and P. Lane. 1998. CD4 T cell cytokine differentiation: the B cell activation molecule, OX40 ligand, instructs CD4 T cells to express interleukin 4 and up-regulates expression of the chemokine receptor, Blr-1. *J. Exp. Med.* 188:297–304. http://dx.doi.org/10.1084/jem.188.2.297

Gerhard, W., K. Mozdzanowska, M. Furchner, G. Washko, and K. Maiese. 1997. Role of the B-cell response in recovery of mice from primary

influenza virus infection. *Immunol. Rev.* 159:95–103. http://dx.doi .org/10.1111/j.1600-065X.1997.tb01009.x

Goins, C.L., C.P. Chappell, R. Shashidharamurthy, P. Selvaraj, and J. Jacob. 2010. Immune complex-mediated enhancement of secondary antibody responses. *J. Immunol.* 184:6293–6298. http://dx.doi.org/10.4049/ jimmunol.0902530

Gururajan, M., J. Jacob, and B. Pulendran. 2007. Toll-like receptor expression and responsiveness of distinct murine splenic and mucosal B-cell subsets. *PLoS ONE.* 2:e863. http://dx.doi.org/10.1371/journal. pone.0000863

Haynes, N.M., C.D. Allen, R. Lesley, K.M. Ansel, N. Killeen, and J.G. Cyster. 2007. Role of CXCR5 and CCR7 in follicular Th cell positioning and appearance of a programmed cell death gene-1high germinal center-associated subpopulation. *J. Immunol.* 179: 5099–5108.

Hildner, K., B.T. Edelson, W.E. Purtha, M. Diamond, H. Matsushita, M. Kohyama, B. Calderon, B.U. Schraml, E.R. Unanue, M.S. Diamond, et al. 2008. Batf3 deficiency reveals a critical role for CD8alpha+ dendritic cells in cytotoxic T cell immunity. *Science.* 322:1097–1100. http://dx.doi.org/10.1126/science.1164206

Huang, N.N., S.B. Han, I.Y. Hwang, and J.H. Kehrl. 2005. B cells productively engage soluble antigen–pulsed dendritic cells: visualization of live-cell dynamics of B cell-dendritic cell interactions. *J. Immunol.* 175:7125–7134.

Jacob, J., G. Kelsoe, K. Rajewsky, and U. Weiss. 1991. Intraclonal generation of antibody mutants in germinal centres. *Nature.* 354:389–392. http://dx.doi.org/10.1038/354389a0

Kasahara, S., and E.A. Clark. 2012. Dendritic cell-associated lectin 2 (DCAL2) defines a distinct CD8α- dendritic cell subset. *J. Leukoc. Biol.* 91:437–448. http://dx.doi.org/10.1189/jlb.0711384

Lahoud, M.H., A.I. Proietto, F. Ahmet, S. Kitsoulis, L. Eidsmo, L. Wu, P. Sathe, S. Pietersz, H.W. Chang, I.D. Walker, et al. 2009. The C-type lectin Clec12A present on mouse and human dendritic cells can serve as a target for antigen delivery and enhancement of antibody responses. *J. Immunol.* 182:7587–7594. http://dx.doi.org/10.4049/ jimmunol.0900464

Lahoud, M.H., F. Ahmet, S. Kitsoulis, S.S. Wan, D. Vremec, C.N. Lee, B. Phipson, W. Shi, G.K. Smyth, A.M. Lew, et al. 2011. Targeting antigen to mouse dendritic cells via Clec9A induces potent CD4 T cell responses biased toward a follicular helper phenotype. *J. Immunol.* 187:842–850. http://dx.doi.org/10.4049/jimmunol.1101176

Le Bon, A., C. Thompson, E. Kamphuis, V. Durand, C. Rossmann, U. Kalinke, and D.F. Tough. 2006. Cutting edge: enhancement of antibody responses through direct stimulation of B and T cells by type I IFN. *J. Immunol.* 176:2074–2078.

Letran, S.E., S.J. Lee, S.M. Atif, S. Uematsu, S. Akira, and S.J. McSorley. 2011. TLR5 functions as an endocytic receptor to enhance flagellin-specific adaptive immunity. *Eur. J. Immunol.* 41:29–38. http://dx.doi .org/10.1002/eji.201040717

Litinskiy, M.B., B. Nardelli, D.M. Hilbert, B. He, A. Schaffer, P. Casali, and A. Cerutti. 2002. DCs induce CD40-independent immunoglobulin class switching through BLyS and APRIL. *Nat. Immunol.* 3:822–829. http://dx.doi.org/10.1038/ni829

Longhi, M.P., C. Trumpfheller, J. Idoyaga, M. Caskey, I. Matos, C. Kluger, A.M. Salazar, M. Colonna, and R.M. Steinman. 2009. Dendritic cells require a systemic type I interferon response to mature and induce CD4+ Th1 immunity with poly IC as adjuvant. *J. Exp. Med.* 206:1589–1602. http://dx.doi.org/10.1084/jem.20090247

McHeyzer-Williams, M., L. McHeyzer-Williams, J. Panus, R. Pogue-Caley, G. Bikah, D. Driver, and M. Eisenbraun. 2003. Helper T-cell-regulated B-cell immunity. *Microbes Infect.* 5:205–212. http://dx.doi .org/10.1016/S1286-4579(03)00012-1

Odegard, J.M., B.R. Marks, L.D. DiPlacido, A.C. Poholek, D.H. Kono, C. Dong, R.A. Flavell, and J. Craft. 2008. ICOS-dependent extrafollicular

helper T cells elicit IgG production via IL–21 in systemic autoimmunity. *J. Exp. Med.* 205:2873–2886. http://dx.doi.org/10.1084/jem.20080840

Pape, K.A., D.M. Catron, A.A. Itano, and M.K. Jenkins. 2007. The humoral immune response is initiated in lymph nodes by B cells that acquire soluble antigen directly in the follicles. *Immunity.* 26:491–502. http://dx.doi.org/10.1016/j.immuni.2007.02.011

Paus, D., T.G. Phan, T.D. Chan, S. Gardam, A. Basten, and R. Brink. 2006. Antigen recognition strength regulates the choice between extrafollicular plasma cell and germinal center B cell differentiation. *J. Exp. Med.* 203:1081–1091. http://dx.doi.org/10.1084/jem.20060087

Pereira, J.P., L.M. Kelly, and J.G. Cyster. 2010. Finding the right niche: B-cell migration in the early phases of T-dependent antibody responses. *Int. Immunol.* 22:413–419. http://dx.doi.org/10.1093/intimm/dxq047

Phan, T.G., J.A. Green, E.E. Gray, Y. Xu, and J.G. Cyster. 2009. Immune complex relay by subcapsular sinus macrophages and noncognate B cells drives antibody affinity maturation. *Nat. Immunol.* 10:786–793. http:// dx.doi.org/10.1038/ni.1745

Qi, H., J.G. Egen, A.Y. Huang, and R.N. Germain. 2006. Extrafollicular activation of lymph node B cells by antigen-bearing dendritic cells. *Science.* 312:1672–1676. http://dx.doi.org/10.1126/science.1125703

Roozendaal, R., T.R. Mempel, L.A. Pitcher, S.F. Gonzalez, A. Verschoor, R.E. Mebius, U.H. von Andrian, and M.C. Carroll. 2009. Conduits mediate transport of low-molecular-weight antigen to lymph node follicles. *Immunity.* 30:264–276. http://dx.doi.org/10.1016/j.immuni .2008.12.014

Rothaeusler, K., and N. Baumgarth. 2010. B-cell fate decisions following influenza virus infection. *Eur. J. Immunol.* 40:366–377. http://dx.doi .org/10.1002/eji.200939798

Saito, T., D.M. Owen, F. Jiang, J. Marcotrigiano, and M. Gale Jr. 2008. Innate immunity induced by composition-dependent RIG-I recognition of hepatitis C virus RNA. *Nature.* 454:523–527. http://dx.doi .org/10.1038/nature07106

Schwab, S.R., and J.G. Cyster. 2007. Finding a way out: lymphocyte egress from lymphoid organs. *Nat. Immunol.* 8:1295–1301. http://dx.doi .org/10.1038/ni1545

Shih, T.A., E. Meffre, M. Roederer, and M.C. Nussenzweig. 2002a. Role of BCR affinity in T cell dependent antibody responses in vivo. *Nat. Immunol.* 3:570–575. http://dx.doi.org/10.1038/ni803

Shih, T.A., M. Roederer, and M.C. Nussenzweig. 2002b. Role of antigen receptor affinity in T cell-independent antibody responses in vivo. *Nat. Immunol.* 3:399–406. http://dx.doi.org/10.1038/ni776

Shiow, L.R., D.B. Rosen, N. Brdicková, Y. Xu, J. An, L.L. Lanier, J.G. Cyster, and M. Matloubian. 2006. CD69 acts downstream of interferon-alpha/beta to inhibit S1P1 and lymphocyte egress from lymphoid organs. *Nature.* 440:540–544. http://dx.doi.org/10.1038/nature04606

Suzuki, K., I. Grigorova, T.G. Phan, L.M. Kelly, and J.G. Cyster. 2009. Visualizing B cell capture of cognate antigen from follicular dendritic cells. *J. Exp. Med.* 206:1485–1493. http://dx.doi.org/10.1084/ jem.20090209

Weir, D.M., L.A. Herzenberg, C. Blackwell, and L.A. Herzenberg. 1986. Handbook of Experimental Immunology. 1:31.6-31.7.

White, A.L., A.L. Tutt, S. James, K.A. Wilkinson, F.V. Castro, S.V. Dixon, J. Hitchcock, M. Khan, A. Al-Shamkhani, A.F. Cunningham, and M.J. Glennie. 2010. Ligation of CD11c during vaccination promotes germinal centre induction and robust humoral responses without adjuvant. *Immunology.* 131:141–151.

Wykes, M., and G. MacPherson. 2000. Dendritic cell-B-cell interaction: dendritic cells provide B cells with CD40-independent proliferation signals and CD40-dependent survival signals. *Immunology.* 100:1–3. http://dx.doi.org/10.1046/j.1365-2567.2000.00044.x

Wykes, M., A. Pombo, C. Jenkins, and G.G. MacPherson. 1998. Dendritic cells interact directly with naive B lymphocytes to transfer antigen and initiate class switching in a primary T-dependent response. *J. Immunol.* 161:1313–1319.